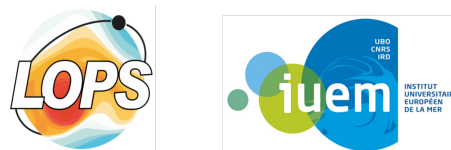


# Mixed layer depth variability in the North Atlantic Ocean in the ARMOR 3D dataset

Lilian Carolina Garcia Oliva

Advisors: Prof. Anne Marie Treguier & Prof. Guillaume Maze

Laboratory for Ocean Physics and Satellite remote sensing (LOPS)  
European Institute for Marine Studies (IUEM)



Master in Environmental Fluid Mechanics  
University Grenoble Alpes  
Grenoble, France  
July, 2020



# Abstract

The mixed layer is the region in the surface of the ocean that is in direct contact with the atmosphere. Because of this, it plays a role as intermediary in the exchange of momentum, heat, gases and fresh water between the atmosphere and the deep ocean. Therefore it is important from, both climatic and biological points of view. It is formed by turbulent mixing of the surface layer of the ocean, driven by heat loss, wind stress and the local circulation. The mixed layer depth is an ocean feature with large spatial and temporal variability.

Therefore, a qualitative description of the spatio-temporal variability of the mixed layer depth is done in this report. This is achieved using the new dataset ARMOR 3D, a high spatial ( $0.25^\circ$ ) and temporal (weekly) database of mixed layer depth. We analyzed the period from 2005 to 2018. The study is focused on the seasonal cycle variability, regarding three regions of the North Atlantic Ocean. These regions are: Gulf Stream, Labrador and Irminger Seas; and North East Atlantic. Each one of these regions has different surface circulation, net heat flux and mixed layer dynamics.

This report covers individual features in each one of the regions, for example the spatial distribution of the temporal variability, for which we find that the areas of large temporal variability are located over areas of deep mixed layers. Regarding the deep mixed layers, we found that they concentrate in specific clusters, i.e., the deep mixed layers of the Labrador Sea have an absolute maximum in the center of the basin. In addition, such deep mixed layer clusters are related to specific features of each one of the regions: to the Gulf Stream, in the Gulf Stream region; to the localized cyclonic circulation, in the Labrador Sea; and to the continental slope, in the case of the North East Atlantic region. For all the three regions, shallow mixed layers were found along the seasonal cycle. The Labrador and Irminger Seas are the region in which the presence of these shallow mixed layers was more evident. Finally, the duration of the processes present during the seasonal cycle: deepening, shoaling and a constant phase of the mixed layer was measured. The maximum MLD is reached, in general, in the final weeks of February and beginning of March. The deepening takes between 6 to 8 months. The shallowing takes around 3 to 4 months and the constant phase, reaching the minimum MLD, between 1 and 3 months.



# Contents

<b>Abstract</b>	<b>iii</b>
<b>1 Introduction</b>	<b>1</b>
1.1 The Ocean Mixed Layer . . . . .	1
1.1.1 Role in the Earth system . . . . .	1
1.1.2 Processes of mixing . . . . .	1
1.2 Importance of the North Atlantic Ocean . . . . .	2
1.3 Objectives of this study . . . . .	3
<b>2 Data</b>	<b>5</b>
2.1 ARMOR 3D dataset . . . . .	5
2.1.1 Spurious Mixed Layer Depth values . . . . .	5
<b>3 Gulf Stream</b>	<b>9</b>
3.1 General presentation . . . . .	9
3.2 Mixed Layer Depth characteristics and seasonal cycle . . . . .	10
3.2.1 Mean and standard deviation . . . . .	10
3.2.2 Amplitude of the seasonal cycle . . . . .	10
3.3 Spatio-temporal statistics of the mixed layer depth . . . . .	11
3.3.1 Dependence of seasonal cycle with latitude . . . . .	11
3.3.2 Mixed layer depth values distribution by seasons . . . . .	12
3.3.3 The seasonal cycle seen from the histograms . . . . .	13
3.4 Summary . . . . .	13
<b>4 Labrador and Irminger Seas</b>	<b>15</b>
4.1 General presentation . . . . .	15
4.2 Mixed Layer characteristics and seasonal cycle . . . . .	16
4.2.1 Mean and standard deviation . . . . .	16
4.2.2 Amplitude of the seasonal cycle . . . . .	16
4.3 Spatio-temporal statistics of the mixed layer depth . . . . .	16
4.3.1 Dependence of the seasonal cycle with longitude . . . . .	16
4.3.2 Mixed layer depth values distribution by seasons . . . . .	18
4.3.3 The seasonal cycle seen from the histograms . . . . .	18
4.4 Summary . . . . .	18
<b>5 North East Atlantic</b>	<b>21</b>
5.1 General presentation . . . . .	21
5.2 Mixed Layer characteristics and seasonal cycle . . . . .	22
5.2.1 Mean and standard deviation . . . . .	22
5.2.2 Amplitude of the seasonal cycle . . . . .	22
5.3 Spatio-temporal statistics of the mixed layer depth . . . . .	23

5.3.1	Dependence of seasonal cycle with latitude . . . . .	23
5.3.2	Mixed layer depth values distribution by seasons . . . . .	23
5.3.3	The seasonal cycle seen from the histograms . . . . .	24
5.4	Summary . . . . .	25
<b>6</b>	<b>Nordic Sea</b>	<b>27</b>
<b>7</b>	<b>Discussion and Conclusions</b>	<b>31</b>
<b>A</b>	<b>Description of ISAS dataset</b>	<b>35</b>
A.1	Comparison of datasets . . . . .	35
A.1.1	Mean Mixed Layer Depth . . . . .	35
A.1.2	Histograms, seasonal cycle . . . . .	37
A.1.3	Seasonal cycles . . . . .	40
	<b>Bibliography</b>	<b>47</b>

# Chapter 1

## Introduction

### 1.1 The Ocean Mixed Layer

The mixed layer (ML) is the region at the surface of the ocean where the temperature, salinity and density are nearly uniform in the vertical. Below the mixed layer, a region of fast change in these properties separates it from the deep ocean. This fast changing region is called thermocline, halocline or pycnocline; if it refers to the temperature, salinity or density. This structure can be seen in Figure 1.1. From 0 m to 100 m depth is possible to see the mixed layer, with nearly vertically constant potential density, temperature and salinity. Under the mixed layer, from 100 m to 200 m, it is possible to see the pycno, halo and thermo-clines, for the three variables. Beyond 200 m it is found the abyssal profile.

The vertical homogeneity of the mixed layer is caused by turbulent mixing processes generated by the interactions between the ocean and the atmosphere. It is through these interactions that fluxes of heat, momentum, fresh water, and other tracers, like  $CO_2$ , are transported to the deep ocean. These interactions make the mixed layer an ocean feature with high temporal and spatial variability [Kantha and Clayson, 2003, Holte et al., 2017].

#### 1.1.1 Role in the Earth system

The mixed layer is important for the long term climate and weather because of its role in the exchange of mass, momentum, energy and heat between the atmosphere and the ocean.

It has biological importance too: it has a role in the food chain, principally in the production of phytoplankton. This is because it is in the mixed layer where the fixation of oxygen, sunlight and the presence of nutrients, transported from the deep ocean, allows the growth of the primary producers. Furthermore, these biological process is important from a climatic point of view. This is because it is during this cycles that carbon fixation occur, making the ocean one of the major sinks of anthropogenic  $CO_2$ . This is also true for the inorganic cycle of carbon. In particular, the  $CO_2$  is absorbed in the cold subpolar areas of the ocean, regions of formation of deep and intermediate waters [Kantha and Clayson, 2003, Talley, 2011, Siedler et al., 2013].

#### 1.1.2 Processes of mixing

The ocean mixed layer is mixed from its top and bottom. At the top, the wind, waves and heat exchanges are the principal agents of mixing. In the bottom, the entrainment driven by large turbulent eddies mixes denser fluid from below into the ML. The impact of these processes on the mixed layer is variable in space and time. The temporal variability can range from diurnal to interannual; including seasonal and intraseasonal variability [de Boyer Montégut et al., 2004]. In

Summer times the MLD can have values of 20 m and Winter, in some areas, be more than 500 m [Monterey and Levitus, 1997, de Boyer Montégut et al., 2004].

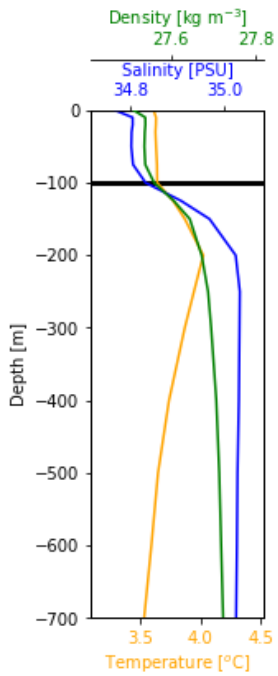


Figure 1.1: November monthly mean of the vertical profile in the point ( $55^{\circ}\text{W}$ ,  $36^{\circ}\text{N}$ ). Potential density, ( $\text{kg m}^{-3}$ ), in green; temperature ( $^{\circ}\text{C}$ ), in yellow; and salinity (PSU) in blue. The black line marks the MLD, 100 m. Monthly mean calculated from ARMOR 3D dataset, over the 2005–2018 period.

layer is deeper in anticyclonic eddies and shallower in cyclonic eddies [Gaube et al., 2019].

## 1.2 Importance of the North Atlantic Ocean

Some parts of the North Atlantic ocean are associated with the conversion of superficial water to denser intermediate and deep waters. This water conversion has an impact in the upper circulation of the Atlantic Ocean: the water mass conversion causes an increase of the northward transport at the Gulf Stream, being, then, a connection between tropical and subtropical waters in direction to the subpolar North Atlantic. This process is the overturning circulation that transports heat to high latitudes in the Atlantic Ocean. The subpolar North Atlantic is a formation site of a type of mode water, the Subpolar Mode Water (SPMW) [Talley, 1996, Talley, 2011].

The deep water that is formed in the North Atlantic Ocean is the North Atlantic Deep Water (NADW). This water mass is a combination of 5 different sources: the Antarctic intermediate Water, the Antarctic Bottom Water, both produced in the south. The other three are formed in the North Atlantic Ocean and they are the Mediterranean Overflow Water (MOW), the Labrador Sea Water (LSW) and the Nordic Sea Overflow Water (NSOW), also known as the Greenland-Iceland-Norwegian Sea Overflow. These water masses are formed in Winter, as a result of intermediate

In the case of the mid-latitudes, the diurnal and seasonal cycles are the most salient modes of the mixed layer variability. This allows us to think that the seasonal variability of the ocean mixed layer depth and heat content are an important factor in air-sea interaction at those latitudes. In this context, the winds play an important role in the variability of the mixed layer depth. For example, during the onset of Spring, the warmer condition re-stratifies the water column. In that period, the mixed layer depth remains almost constant once the shallow Spring-Summer thermocline forms. It is during this period that the wind events have a strong influence. In contrast, during Autumn, the wind and heat forcing control the deepening of the mixed layer. In this period, the passing of big storms deepens the mixed layer because they cause large heat loss at the surface of the ocean.

Sensible and latent heat fluxes are a big source of variability of mixed layer depth, changing the temperature of the surface of the ocean. Also important are the precipitation events, that impact the temperature and change the surface salinity, increasing the buoyancy of the surface, inhibiting turbulent mixing [Kantha and Clayson, 2003, McCulloch et al., 2004, Talley, 2011].

One more source of spatial and temporal variability is the mesoscale eddy activity in the ocean. It has been documented that the mixed

convection driven by local heat loss; therefore, through the mixed layer dynamics [Talley, 1996, Talley, 2011].

Under this perspective, it is important to understand the variability of the mixed layer depth over the North Atlantic Ocean, and more importantly, over the formation sites of these water masses. To do this, instead of making a large scale study, considering the complete North Atlantic, three smaller regions were chosen. The criterion was, basically, to identify regions in which the Winter deepening of the mixed layer reaches maximum values that represent an important contribution to the deep water formation.

The regions chosen are: 1) Gulf Stream, 2) Labrador and Irminger Seas, 3) North East Atlantic, and 4) Nordic Sea (see Chapter 6 where the plots are presented, but not discussed); the regions are delimited in Figure 1.2. Inside each region were also selected the areas where the deepest mixed layers are reported. These sub-regions are delimited by colored squares: Gulf Stream Extension (blue); Labrador Sea (black); Irminger Sea (pink); South Rockall Trough (orange); Nordic Sea North (white) and Nordic Sea South (cyan).

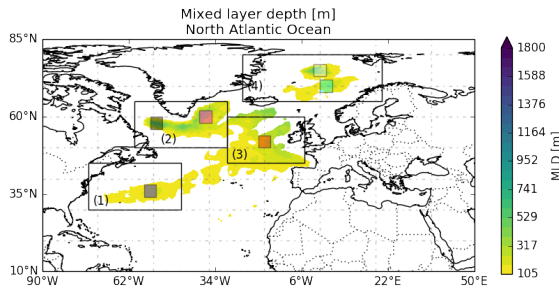


Figure 1.2: Monthly mean of the Mixed Layer depth for March in the North Atlantic Ocean. The mean is computed over the 2005-2018 period. The bounded regions are: 1) Gulf Stream, 2) Labrador and Irminger Seas and 3) North East Atlantic and 4) Nordic Sea (extra).

Each one of the regions has its own characteristic surface and deep dynamics. Because the regions are at different locations they have different surface forcing, thus different development of the mixed layer. Some examples these differences are: the interannual variability, the timing and maximum value of the MLD and the smoothness of the cycle per se (Figure 1.3).

### 1.3 Objectives of this study

Due to the large temporal and spatial variability of the mixed layer depth, it is important to understand, document and quantify how the local circulation patterns, bathymetry and dynamics, shape the spatial distribution of the mixed layer depth in different regions; and how this spatial distribution changes in time.

Therefore, this study will be focused on the description of:

- The seasonal cycle of the mixed layer depth,
- The spatial variability of the seasonal cycle,
- The mean surface currents and eddy variability effects on the mean state and variability of the mixed layer depth.

These points will be developed individually for each one of the chosen regions: Gulf Stream Extension, Labrador and Irminger Seas and North East Atlantic. After this individual description a comparison of the regions will be done.

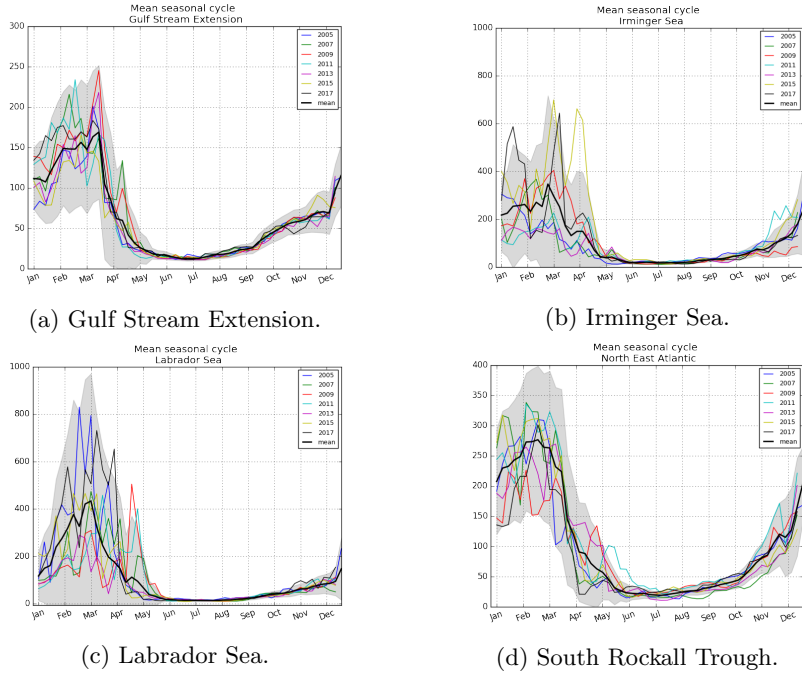


Figure 1.3: Mean seasonal cycle over the Gulf Stream Extension, Irminger Sea, Labrador Sea and South Rockall Trough sub-regions (in black) and standard deviation (gray shades). In color seasonal cycle for some years, inside each sub-region. The mean was computed over the 2005-2018 period.

This report is organized as follows: chapter 2 describes the dataset used. The chapters 3, 4 and 5 cover each one of the regions: Gulf Stream, Labrador and Irminger Seas and North East Atlantic, respectively. A small summary is written at the final of each chapter. The discussion and conclusions are presented in chapter 7. As an additional content a set of figures for the Nordic Seas are presented in the chapter 6. These figures are the same as for the other regions, though the description and analysis is absent.

# Chapter 2

## Data

### 2.1 ARMOR 3D dataset

The data used in this report are extracted from the ARMOR 3D dataset [Guinehut et al., 2012]. It is a database that includes a 2D Mixed Layer Depth (MLD) field and 3D fields of geopotential height, geostrophic velocity, density and temperature as well. It is the product of the statistical merging between in situ and satellite ocean observations. This merging was achieved through multiple and simple linear regression methods that derive temperature and salinity fields from sea level altimetry (SLA) and sea surface temperature (SST). This process takes into account the covariances and the mean values of the fields calculated from historical in situ observations [Guinehut et al., 2012, Verbrugge et al., 2019].

The idea behind the development of this dataset is to take advantage of the high accuracy of the salinity and temperature profiles (from Argo) and the high resolution of satellite altimeter and sea surface temperature, and thus, generate a high temporal and spatial resolution 3D global thermohaline field. The Mixed Layer Depth is estimated using a variable threshold on density, as done by [de Boyer Montégut et al., 2004]; this density criterion is equivalent to a temperature difference of 0.2 °C in the local temperature with respect to the surface.

ARMOR 3D has a spatial resolution of 0.25° in a regular grid. The vertical sampling is done over 33 levels, from 0m to 5500m; having a bigger resolution in the first 50m. The temporal resolution is weekly, over a period from January 1993 to December 2018 [Guinehut et al., 2012, Verbrugge et al., 2019]. In this study, the period used is 2005-2018; period in which the coverage of ARGO profiles is considered to be good.

#### 2.1.1 Spurious Mixed Layer Depth values

During the realization of this work, a problem related to extremely deep mixed layers in the dataset was found. This was especially noticeable in the Gulf Stream region. In this region, the mixed layer values reported by the ARMOR 3D reached 4000m and it is already well documented that the maximum values are around 600m [Holte et al., 2017]. These differences between the data and the reported values indicate that there was a problem with the data. This problem was found in the entire time series. It affected several grid points spread across the entire region, sometimes in small clusters. After the time averaging or standard deviation computation, these extreme spurious values were still present in the dataset. Both situations are plotted in the Figures 2.1 and 2.2. In Figure 2.1a it is possible to see the time standard deviation of the MLD in the original dataset. We see a cluster of high standard deviation in the region bounded by (50°, 45°)W, (40°, 42°)N. The maximum value of standard deviation is found at the point (47.8°W, 41.3°N), whose time series is plotted in Figure 2.2a. At this grid point, the MLD reaches values larger than 1000m during the Winter times.

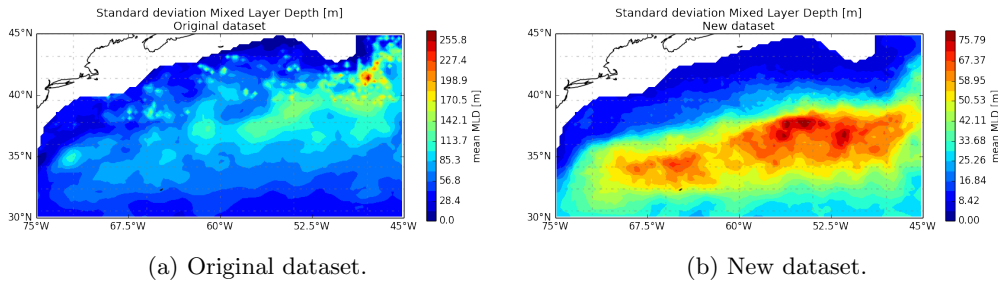


Figure 2.1: Standard deviation in the Gulf Stream region. (a) Original dataset. (b) New dataset. Note that the color scale is different for both plots. The standard deviation is calculated in a 2005–2018 period.

Because of this, it was needed to filter the dataset from this spurious grid points. Thus, the first idea to do it was to discriminate grid points comparing them with the wintertime (January, February, March) mean plus three standard deviation ( $M\bar{L}D + n\sigma_{MLD}$ ), where  $n = 3.0$  (cyan line in Figure 2.2a).

The criterion was applied to the complete time series in order take out the extreme values that may be outside of the Winter time as well. After applying this filter the grid points loss was too large. In Figure 2.3 can be seen that the impact of the filter is large at some time steps. Because of this, the filtering method was not applied.

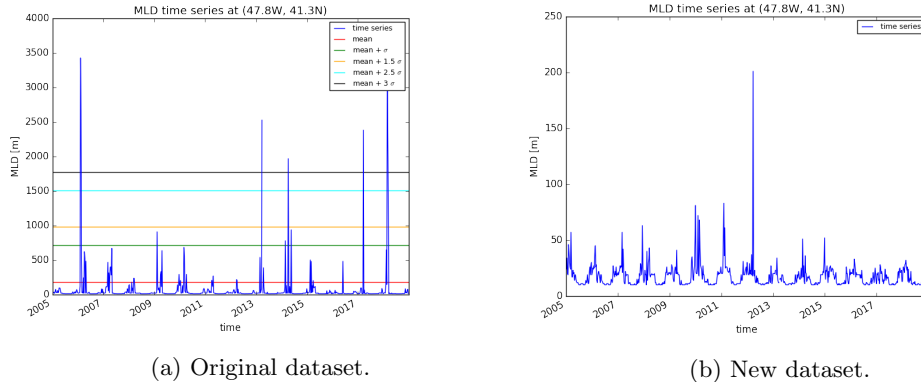


Figure 2.2: Time series (blue) of the grid point (47.8°W, 41.3°N). (a) Original dataset. Horizontal lines marking the mean (red); mean+1.0 $\sigma$  (green); mean+1.5 $\sigma$  (yellow); mean+2.5 $\sigma$  (cyan) and mean+3.0 $\sigma$  (black). (b) Time series (blue) from the new dataset. Note that the color scale is different for each plot.

After a short communication (by e-mail) with Nathalie Verbrugge (CLS), part of the ARMOR 3D developing group, we were informed that this was a problem that was not reported before. In fact, this dataset has already been used in the intercomparison project by [Toyoda et al., 2017]. Nevertheless, due to the global and monthly scales of the study, this problem with the extreme MLD values was not reported. Following the discovery of the problem, a new MLD field was generated by the ARMOR 3D team. This new dataset has a smoother field, with MLD values do not go beyond 100 m, but occasionally (Figures 2.1b and 2.2b)

This new dataset makes use of a different criterion to calculate the mixed layer depth, always based in the [de Boyer Montégut et al., 2004] methodology. The difference between the MLD estimation of the new field and the original one (previously described) is that along with the density-based criterion, a temperature-based criterion was used. The reported MLD value is the smaller

of these two values. This is the dataset that is used in this report.

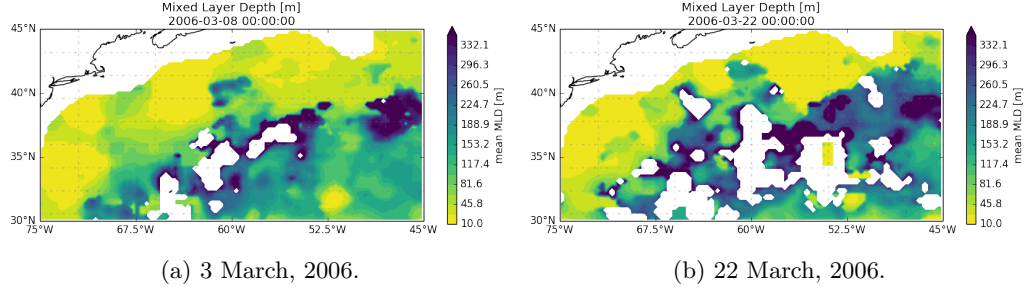


Figure 2.3: Grid point loss using the filter with the condition  $\bar{x} + 3\sigma$ . For the time steps in March of 2006.

The description of the regions include the net heat flux  $\text{W m}^{-2}$  at the surface of the ocean. The net heat flux is defined as the sum of: latent heat flux, net solar radiation, net thermal radiation and sensible heat flux. Along with the heat flux, the bathymetry was also included, this dataset was obtained from monthly averaged reanalysis ERA5. The bathymetry dataset was obtained from GEBCO Compilation Group [Group, 2020].

Finally, because the focus of the study is in the deep ocean, a bathymetric filter was applied. Thus, the gridpoints that reach depths greater than 2000 m were considered in the study. The processing of this dataset was done using Python and Jupyter notebooks. All the code needed for the processing and visualization of the results was newly developed for this study. This resulted in the implementation of 10 different routines. This work is documented and available in the Git Hub repository <https://github.com/LilianGO/MLD-Project>. Each of the products of the analysis is organized in separate regions, which will be described in the following sections.



# Chapter 3

## Gulf Stream

### 3.1 General presentation

The region of the Gulf Stream Extension refers to the area occupied by the continuation of the Western Boundary current at the north of the Florida Straits and that continues into the north-eastern side, flowing to the North Atlantic Ocean. It is a region characterized by a very strong current (reaching velocities up to  $150 \text{ cm s}^{-1}$ ), in terms of transport (between  $60 \text{ Sv}$  to  $100 \text{ Sv}$ , varying meridionally) and a strong eddy variability. The current transports warm and saline surface waters from the warm subtropical latitudes to the cold subpolar regions [Talley, 2011].

The Gulf Stream is also associated with the formation of the Eighteen Degree Waters (EDW), also known as North Atlantic Subtropical Mode Water (NASTMW). This Mode Water (MW) arises from convective activity in the thickened mixed layers at the south of the Gulf Stream. This formation is associated with large surface heat loss during Winter. This heat loss is the result of cold and dry outbreaks of wind over the area coming from the neighboring continental masses [Talley, 2011].

To have a view of the general surface circulation of the Gulf Stream, the Sea Surface Height (SSH) time mean and standard deviation is used. From geostrophy, it is known that the SSH horizontal gradient is related to the horizontal components of velocity. It is evident that the region is divided by the strong current (given by the strong gradient) flowing north-east ward. This is the Gulf Stream. Along this current, it can also be spotted small regions of strong variability (std ranging from 10 cm to almost 0.5 m). These regions of high variability are associated with the eddy activity of the Gulf Stream (Figure 3.1a). In terms of heat flux, in Figure 3.1b, it is seen that in average, the Gulf Stream is a region of strong heat loss.

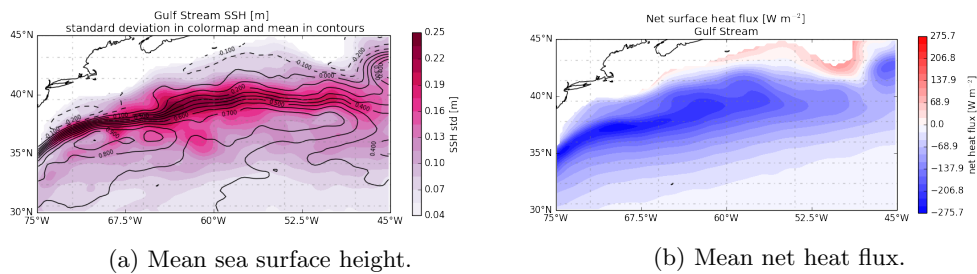


Figure 3.1: Gulf Stream: (a) Average and standard deviation of the sea surface height, SSH [m]. Contours represent the mean and color shading the standard deviation. (b) Net surface heat flux [ $\text{W m}^{-2}$ ]. Blue color shading represents flux out of the ocean and red flux into. Both fields computed over 2005-2018.

The vertical structure of the Gulf Stream has changes in the meridional direction. For example, Figure 3.2 shows the potential density profiles along a meridional section, across the Gulf stream, at 60°W. Going in the northward direction it is possible to see a strong gradient over the latitudinal section of the Gulf Stream. This sharp transition is often called the “North Wall” of the Gulf Stream [Talley, 2011]. Further, there is a strong vertical density gradient at the northern side of the Gulf Stream.

## 3.2 Mixed Layer Depth characteristics and seasonal cycle

### 3.2.1 Mean and standard deviation

To have a first look at the mixed layer depth in the Gulf Stream, a time average and standard deviation were computed. The objective of this is to identify the areas in the region that have the largest time variability and to have a first idea of the spatial distribution of these changes. The resulting plot is in Figure 3.3.

It can be noticed that the Gulf Stream acts as a barrier between deep and shallow values of average MLD: shallow at the north, deep at the south. There can be identified two hot spots of deep mixed layer. One is located near (63°W, 35°N), with MLD values of  $(62 \pm 64)$  m. The other is located at (55°W, 37°N), with MLD around  $(72 \pm 80)$  m.

These two hot spots correspond to the formation site of two kinds of EDW. The first one located at 73°W to 63°W and 35°N, which forms warmer and salty waters ( $18^{\circ}\text{C}$  and 36.6 PSU); and the other fresher and colder waters, located around 55°W [Joyce, 2011].

It is important to point out that going into the deep mixed layer values, the standard deviation gets as large as the MLD mean. This description fits with the already discussed description of the isopycnals in the north-south direction, in Figure 3.2. Comparing the distribution of the average MLD and the isopycnals, it can be noticed that the maximum MLD values are located over the latitudes south of the Gulf Stream. The weak stratification in that region is correlated to the development of deep mixed layers, located at the south of the current.

When the time mean MLD (Figure 3.3) with the mean net heat flux (Figure 3.1b) it appears that the regions with deep mixed layers coincide with the large heat loss areas. Despite this spatial similarity, the maximum MLD values do not coincide with the maximum heat loss.

### 3.2.2 Amplitude of the seasonal cycle

From the typical seasonal cycle in the previous section, in Figure 1.3a, and from previous work in the topic, it is known that the deepest MLD values are about  $(160 \pm 10)$  m [Schiller and Ridgway, 2013], reaching, in some points, maximum values of about 600 m as reported by [Holte et al., 2017].

To do so, it was necessary to plot the average amplitude of the seasonal cycle. This mean seasonal cycle was computed as follows: for each grid point, the amplitude of each year’s cycle was calculated. The amplitude was defined as the difference between the deepest weekly value and the

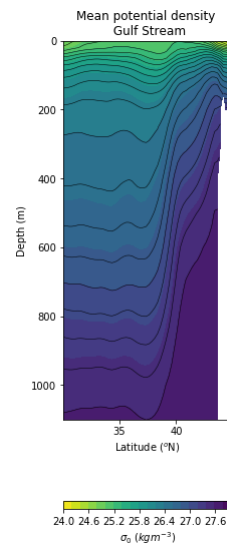


Figure 3.2: Meridional section of potential density across the Gulf stream, at 60°W. The average was computed over 2005-2018 period.

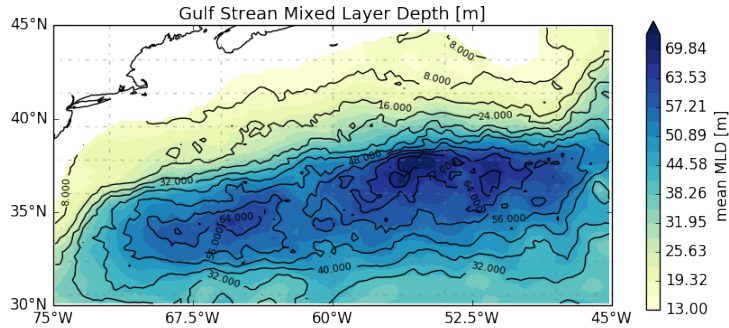


Figure 3.3: Time average and standard deviation of the Mixed Layer Depth, MLD [m]. Contours represent the mean and color shading the standard deviation. The plot shows only areas deeper than 2000 m. In red contours the time average of SSH [m], shows the position of the Gulf Stream. All mean fields are computed over 2005-2018.

shallowest weekly values, for each one of the years; then the average value was calculated. The result is shown in the Figure 3.4.

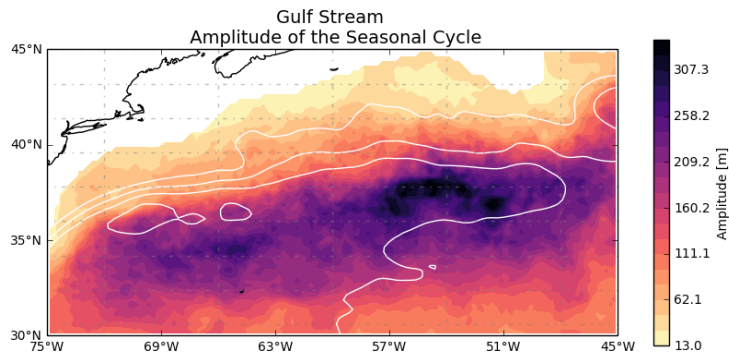


Figure 3.4: Mean amplitude of the seasonal cycle, in meters. The plot shows only areas deeper than 2000 m. In white contours the time average of SSH [m], shows the position of the Gulf Stream. Both fields are computed over 2005-2018.

By looking at Figures 3.3 and 3.4, it is possible to see that the amplitude of the seasonal cycle tends to have the same distribution of the mean mixed layer depth. The Gulf Stream acts as a barrier dividing large amplitude from small amplitude of the seasonal cycle: two amplitude hot spots can be identified at the south of the Gulf Stream. These hot spots correspond to the EDW formation sites.

### 3.3 Spatio-temporal statistics of the mixed layer depth

#### 3.3.1 Dependence of seasonal cycle with latitude

The dependence of the seasonal cycle with the latitude is evaluated here. To analyze this, a Hovmöller plot was built. This plot considers the zonal average of the seasonal cycle in the Gulf Stream region. As a reference, a white line is drawn to indicate the mean position of the Gulf Stream. This was estimated as the maximum meridional SSH gradient at 60°W. The time axis is shifted, starting from July, to make a special emphasis onto the winter months. The result is presented in Figure 3.5.

Figure 3.5 reinforces the idea of the division made by the Gulf Stream. At the north of  $40^{\circ}\text{N}$  the seasonal cycle is not as strong as at the southern latitudes. And the maximum zonal values are localized around  $35^{\circ}\text{N}$ , at the end of the winter.

The restratification process is faster than the destratification (Figure 3.5). The difference between north-south of the Gulf Stream is also noticeable. At the north, the destratification has a delay of three months, compared with the south. The former starts at mid-October and the latter at the final of July. In the case of the restratification, the process seems to have the same duration, starting in late March and finishing around June.

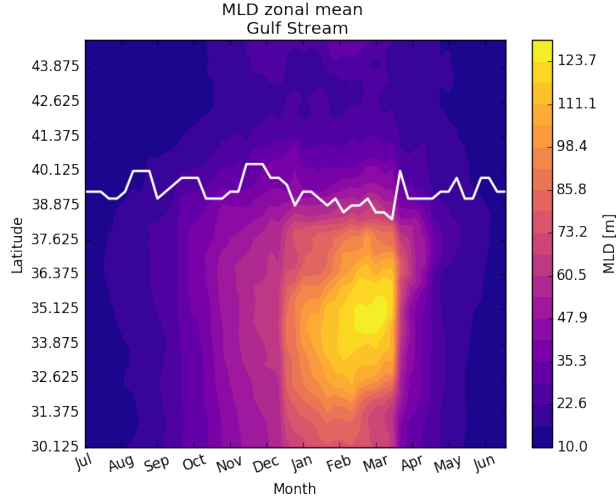


Figure 3.5: Zonal mean seasonal cycle of the MLD [m]. The mean is computed from weekly values for the years from 2005 to 2018. In white line the mean position of the Gulf Stream at  $60^{\circ}\text{W}$ , calculated as the maximum meridional SSH gradient. The plot shows only areas deeper than 2000 m.

### 3.3.2 Mixed layer depth values distribution by seasons

The regional spatial heterogeneity of the MLD in each season was evaluated using histograms, in Figure 3.6. These histograms account for the number of grid points, in the entire dataset, at a given depth bin. In each of the cases, the grid points are separated by season, each one identified by a color. The seasons are chosen, as follows: Winter, 'JFM' (blue); Spring, 'AMJ' (green); Summer, 'JAS' (red); and Autumn 'OND' (yellow). Both of the histograms are normalized.

Therefore, the histogram in Figure 3.6a, in semi-log scale, counts the contribution of each season in the distribution of the mixed layer depth in the region. Due to the large skewness of the data, it was necessary to use a logarithmic scale in the y-axis. This was done in order to visualize all the counts at the deepest values of the mixed layer. Finally, the cumulative histogram is shown in the Figure 3.6b.

It seems that 50% of the total grid points are in the first 25 m; and up to the 90% of the data accounts for MLD of 100 m. The seasons that contribute the most to the first 50% are Summer and Autumn, as shown in the Figure 3.6b. The remaining 10% of the mixed layer, from 100 m to 600 m, occurs in the Spring and Winter seasons; the depths beyond 200 m represent less than 1% of the total data (Figure 3.6b).

Looking individually at the distribution by seasons, in Figure 3.6a, is noticeable that: in Summer, Winter and Spring, the mode is in the first 15 m; in the case of Autumn, the mode is located between 20 m to 60 m. During Winter and Spring there are two local peaks at the tail

of the histograms. One around 400 m and other at 500 m, although a fraction of the total grid points is of order  $10^{-4}$  or less. The distribution of Spring is very similar to the one in Summer, in the first 25 m. This means that during Spring, there are mixed layers that were already stratified. This fast restratification can explain the difference in number of grid points between Winter and Spring, in the 30 m to 480 m depths.

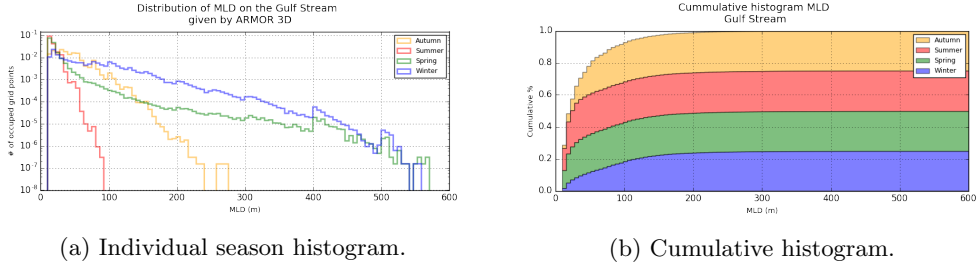


Figure 3.6: (a) Normalized histogram of the MLD discriminated by seasons, in semi-log scale. (b) Normalized cumulative histogram for each one of the seasons. The seasons are identified by colors: Summer (red), Autumn (yellow), Winter (blue) and Spring (green). Both histograms consider each one of the 730 time steps in the 2005-2018 period, for the complete region. The total number of grid points is 4396806.

### 3.3.3 The seasonal cycle seen from the histograms

To have a better understanding of the evolution of the mixed layer distribution in the region, a mixed-layer-depth/time-dependent plot for the seasonal cycle was constructed. The result of this is in the Figure 3.7, where the colorbar is in logarithmic scale, denoting the number of grid points  $N$  in each pair (time, MLD).

It can be seen that in the Gulf Stream region, the diversity of mixed layer depths is strongly modulated by the seasonal cycle (Figure 3.7). And that the most homogeneous period is in the month of June. It is also possible to identify two different groups of MLD. Each group represented as one maximum, both of order around  $10^2$ , in the distribution. One of this maxima stays at the shallow MLD values, along the complete cycle. The second group has a larger journey in along the depths. The maximum that identifies this group vanishes at the beginning of February and is recovered at middle March. The presence of these two groups of MLD agrees with the previous description of the region: small amplitude seasonal cycle MLD at the north of the Gulf Stream and large amplitude seasonal cycle at the south.

## 3.4 Summary

In the Gulf Stream Extension region, the meridional distribution of the mixed layer depth is influenced by the position of the Gulf Stream: deep MLD are at the south and shallow MLD are at the north, with respect to the Gulf Stream. This distribution also matches with the meridional section of the potential density across the Gulf Stream.

In terms of temporal mean and standard deviation of the MLD, the distribution is also set by the position of the Gulf Stream. The large mean MLD values are accompanied by also large variability. These large values are concentrated in two hot spots. One extends in the area from  $73^{\circ}\text{W}$  to  $63^{\circ}\text{W}$  at latitude  $35^{\circ}\text{N}$ , with the value  $(62 \pm 64)$  m. The other located around  $55^{\circ}\text{W}$  reaches  $(72 \pm 80)$  m. Both hot spots are related to EDW formation [Joyce, 2011].

The seasonal cycle has the same distribution as the mean values. The small amplitudes are at the north of the Gulf Stream, with values from 13.0 m to 62.0 m. On the other hand, the large

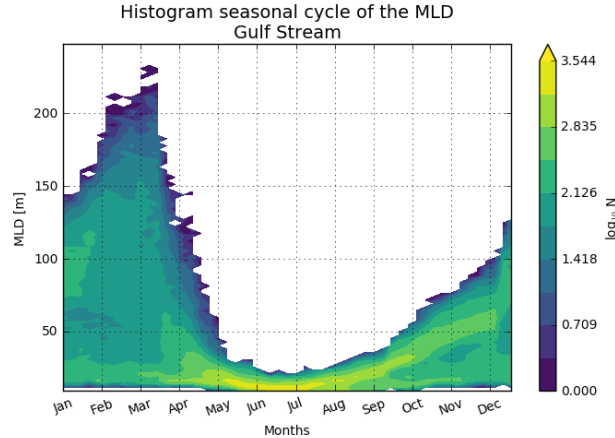


Figure 3.7: Seasonal cycle of the MLD PDF over the Gulf Stream, represented as weekly average over the period of 2005-2018. The x-axis is in months, y-axis is the Mixed Layer Depth. The colormap, in log scale, indicates the number of grid points  $N$  with a given MLD value at a given time.

seasonal amplitude are at the south. They range from 150.0 m to 350.0 m. The hot spots are also noticeable. The hot spot located at 55°W has the largest MLD seasonal amplitude.

The seasonal cycle of the MLD changes with latitude. The most noticeable feature is the timing in which the maximum MLD is reached, as well as the differences between the destratification and restratification of the vertical profile. The difference between the north and south of the Gulf Stream is again present. In the north, the mixing starts at mid-October, the maximum is in the middle of March and the restratification ends in May. In the south, the mixing starts in the first weeks of August. This is also noticeable from the histograms of MLD values in the region. The maximum is reached at the beginning of March. The mixing takes around 8 months. The restratification starts in the second half of March and finishes in June.

# Chapter 4

## Labrador and Irminger Seas

### 4.1 General presentation

The Labrador and Irminger Seas (and their associated currents) form part of the western part of the subpolar gyre of the North Atlantic Ocean. The Labrador Sea has been known as a region of intermediate water formation, the Labrador Sea Water (LSW). The LSW is characterized by low temperature, low salinity (around  $2.9^{\circ}\text{C}$  to  $3.0^{\circ}\text{C}$ , 34.84 PSU and  $27.78\text{ kg m}^{-3}$ ) [Pickart et al., 2003] and high dissolved gases, like oxygen. This water mass is formed by deep convection and contributes to the Atlantic Overturning Circulation. Its importance lies in the impact that the changes in its properties affect the absorption of atmospheric gases, like the carbon dioxide ( $\text{CO}_2$ ) [Talley and McCartney, 1982, Lazier et al., 2002, Talley, 2011, Holte et al., 2017].

Recent studies have pointed the Irminger Sea as a LSW formation site. This formation is tied to specific conditions, like: positive North Atlantic Oscillation (NAO) index, strong heat loss due to high-speed winds and preconditioning of the water column [Bacon et al., 2003, Pickart et al., 2003, Piron et al., 2016].

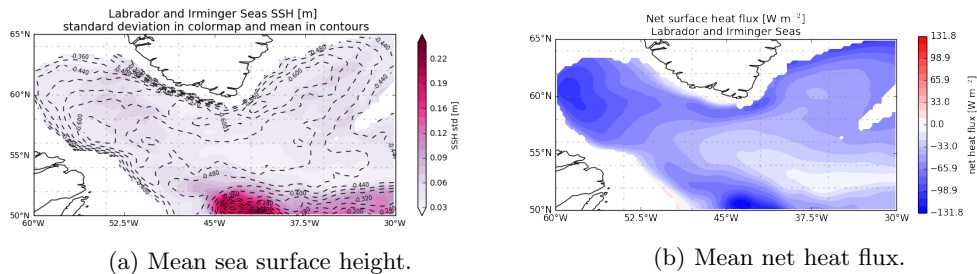


Figure 4.1: Labrador and Irminger Seas: (a) Average and standard deviation of the sea surface height, SSH [m]. Contours represent the mean and color shading the standard deviation. (b) Net surface heat flux [ $\text{W m}^{-2}$ ]. Blue color shading represents flux out of the ocean and red flux into. Both fields computed over 2005-2018.

The general circulation of this region is dominated by low SSH. It has a minimum of SSH at the center of both Labrador and Irminger Seas (Figure 4.1a). For example, the minimum in the Labrador Sea reaches a SSH of  $-0.6\text{ m}$ , located around  $(55^{\circ}\text{W}, 56^{\circ}\text{N})$ . In the Irminger Sea, the minimum of an approximate value of  $-0.6\text{ m}$  is spread along the southern part of the sea and in between of the two subregions. This SSH minimum values indicate, by geostrophy, that the region is characterized by cyclonic circulations. Analyzing the standard deviations is possible to state that the region is quite stable. The complete region experiments net cooling (Figure 3.1b). The larger heat loss is located at the Labrador sea, reaching a flux approximate to  $-115\text{ W m}^{-2}$ . In the

other hand, in the Irminger Sea, the heat loss is smaller, having a minimum of around  $-50 \text{ W m}^{-2}$ . In the central part, between both seas, the heat loss-gain is almost null.

## 4.2 Mixed Layer characteristics and seasonal cycle

### 4.2.1 Mean and standard deviation

The distribution of the MLD concentrates the deepest values at the point ( $53^\circ\text{W}$ ,  $57^\circ\text{N}$ ), in the center of the Labrador Sea. Eastward of the Labrador Sea, at  $45^\circ\text{W}$ , there are also maximum MLD values matching with the description provided by [Holte et al., 2017]. The Irminger Sea has sector of deep MLD too; it is located approximately at  $37^\circ\text{W}$ . Furthermore, the variability of the MLD in time follows the distribution of the mean MLD. Finally, the spatial distribution of the MLD maxima corresponds to the spatial distribution of the minimum in SSH, in Figures 4.2 and 4.1a.

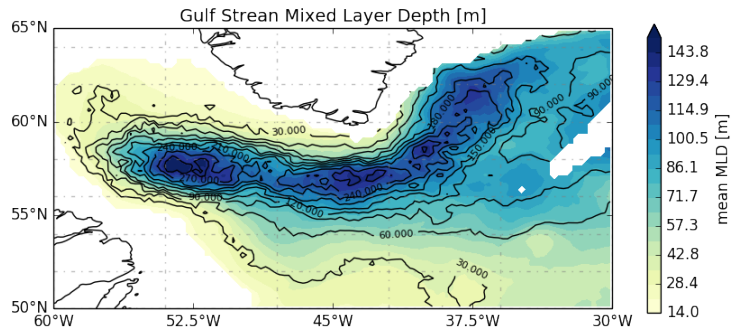


Figure 4.2: Time average and standard deviation of the Mixed Layer Depth, MLD [m]. The average is plotted in colormap and the standard deviation in contours, these quantities are computed in the 2005-2018 period.

### 4.2.2 Amplitude of the seasonal cycle

The maximum mean values of MLD in the sub-regions of deepest mixed layers can reach 1000 m in the Labrador Sea; and 750 m in the Irminger Sea (Figures 1.3c and 1.3b). The literature reports values of maximum MLD 800 m to 1800 m in the Labrador Sea [Talley, 2011, Holte et al., 2017]. For the Irminger Sea, the values can be larger than 800 m [Holte et al., 2017]. All of these maxima MLD are reported in the winter times. The average amplitude of the cycle was calculated and plotted in Figure 4.3.

A hot spot of large MLD seasonal cycle is at the center of the Labrador Sea, centered at ( $53^\circ\text{W}$ ,  $57^\circ\text{N}$ ), in Figure 4.3. It has an amplitude of 1450 m. In general, the amplitude of the seasonal cycle decreases going out of the hot spot, where the minimum values have the same magnitude as the mean MLD. Going eastward, to the Irminger Sea, the amplitude of the seasonal cycle is around 900 m. The amplitude of the seasonal cycle shares the same spatial distribution as the mean and standard deviation of MLD.

## 4.3 Spatio-temporal statistics of the mixed layer depth

### 4.3.1 Dependence of the seasonal cycle with longitude

Due to the spatial configuration of this region, it was chosen to analyze the zonal dependence of the seasonal cycle. The resulting plot is in Figure 4.4.

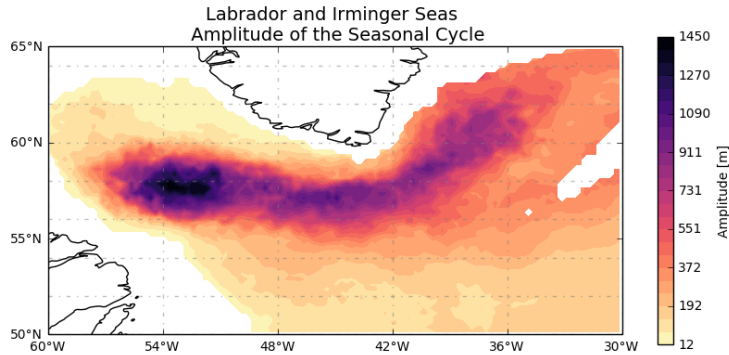


Figure 4.3: Mean amplitude of the seasonal cycle, in meters, computed for the years from 2005 to 2018.

The region has three different maxima, all happening between January to the end of March, see Figure 5.4. The maxima are located at 55°W, 45°W and 36°W. These maxima correspond to the mean maxima found in Figure 4.2. Therefore, these maxima correspond to the Labrador Sea, between both seas and for the Irminger Sea; respectively.

The deepening of the mixed layer in the Labrador Sea is longer than in the Irminger Sea.

Going eastward, starting from the Labrador Sea, the deepening of the mixed layer begins earlier. At the western region the deepening starts in early October, and in the eastern sites it starts in September. In the case of the maxima, it is seen that the Labrador Sea has a double peak, separated by almost a month. Happening at beginning of February and March, respectively. In the case of the inter-sea section, the maximum is reached once, at the final of February. For the Irminger Sea, the maximum is slowly reached and it happens in late February. The shoaling of the mixed layer starts at the same time in all the sections, at the second half of March. The minimum MLD values are reached at the beginning of May; in the western section is in the first weeks, and going to the east this process ends at mid-May.

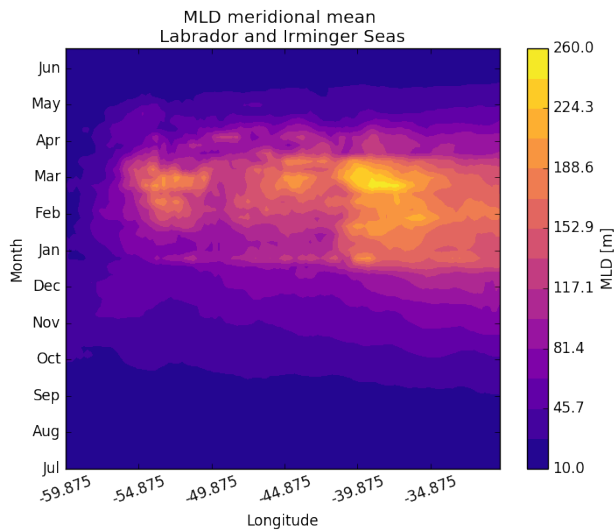
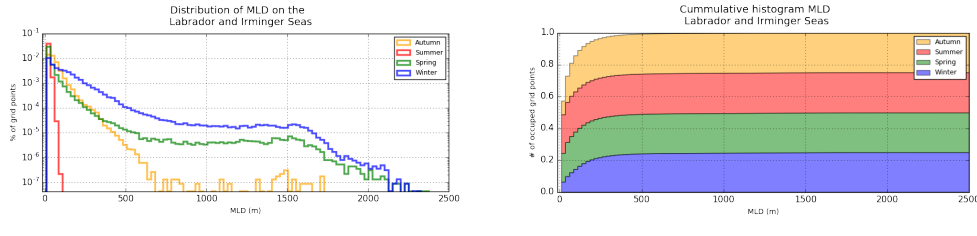


Figure 4.4: Meridional mean seasonal cycle of the MLD [m] over the Labrador and Irminger Seas. The mean is computed from weekly values for the years from 2005 to 2018.

### 4.3.2 Mixed layer depth values distribution by seasons

The histogram in Figure 4.5b counts the contribution of each season in the complete distribution of the mixed layer depth over the region. Almost 60% of the total grid points are in the first 35 m. Up to the 90% of the data accounts for MLD of 135 m. The seasons that contribute the most to the first 60% are Summer and Spring (with most of the grid points), as shown in Figure 4.5a. In Autumn start to appear MLD larger than 500 m. The remaining 10% of the mixed layer depths, from 135 m to 2300 m, occurs in the Spring and Winter seasons. The depths beyond 200 m are less than 6% of the total data.

Looking individually at the distribution by seasons, in Figure 4.5a, is noticeable that: in Summer, Winter and Spring, the mode is in the first 35 m. During Winter, Autumn and Spring there is one maximum at the tail of the histogram, around 1500 m, although ratio out of total grid points is in the order of  $10^{-5}$  or less. In the first 35 m the distribution of Spring is very similar to the one of Summer. This means that during Spring, there are points that already returned to its minimum depth. This would explain the difference between Winter and Spring at the depths 60 m to 2500 m.



(a) Individual season histogram.

(b) Cumulative histogram.

Figure 4.5: (a) Normalized histogram of the MLD discriminated by seasons, in semi-log scale. (b) Normalized histogram for each one of the seasons. The seasons are identified by colors: Summer (red), Autumn (yellow), Winter (blue) and Spring (green). Both histograms consider each one of the 730 time steps in the 2005-2018 period, for the complete region.

### 4.3.3 The seasonal cycle seen from the histograms

The distribution of the MLD values in this region has a permanent maximum in the shallow values, in Figure 4.6. The magnitude of this maximum is affected by the seasonal cycle, being the smallest during Winter and the larger during Summer. This permanent maximum indicates that inside this region the MLD remains shallow at some locations.

In general terms, the PDF seasonal cycle evolves as follows: in winter months, the MLD values reach their maximum value at the end of February, when also the histogram is wider. The MLD starts to get shallow at the beginning of March. This is a very sudden contraction. The MLD keeps getting shallow all along Spring until the start of Summer, in July, when the grid points are concentrated in the shallowest MLD values. This peak is maintained during all Summer. In September, the MLD starts to deepen, therefore the histogram starts to widen.

## 4.4 Summary

In this region the distribution of the MLD is located at the center of the Labrador and Irminger seas, matching with the distribution of the cyclonic circulations inside the sea basins.

Therefore, time standard deviation and amplitude of the seasonal cycle have a similar distribution. The maximum values are concentrated in two well-defined areas: Labrador and Irminger Seas. The larger MLD mean and variability are in the Labrador Sea. The average MLD values are

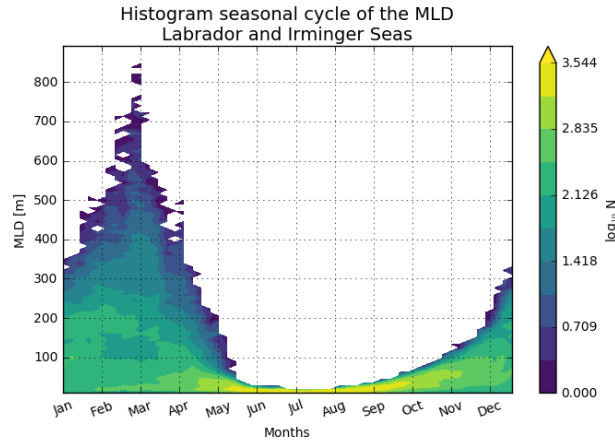


Figure 4.6: Seasonal cycle of the mixed layer depth histogram over the Labrador and Irminger Seas, represented as weekly average over the period of 2005-2018. The x-axis is in months, y-axis is the Mixed Layer Depth. The colormap, in log scale, indicates the number of grid points  $N$  with a given MLD value.

$(172 \pm 300)$  m in Labrador Sea and  $(128 \pm 200)$  m in Irminger Sea. The amplitude, in the other hand reaches values of 1450 m in the Labrador sea and in the Irminger Sea 900 m.

The seasonal cycle has differences in the zonal direction. This is reflected in the timing in the beginning and end of the deepening of the MLD and the following restratification. In the Labrador Sea, along  $55^{\circ}\text{W}$ , the deepening starts around the last weeks of September reaching the maximum MLD at the beginning of March. The restratification in the same longitude starts after the first weeks of March reaching the minimum MLD values at the beginning of May. So, the mixing takes an approximate of 6 months and the restratification, 3 months. At the Irminger Sea, at  $37^{\circ}\text{W}$ , the destratification starts at the first weeks of September, reaching the maximum in late February; the restratification takes place from March to late April.



# Chapter 5

## North East Atlantic

### 5.1 General presentation

The North East Atlantic region is an area over which the North Atlantic Current (NAC) passes. The NAC flows eastward on the southern side of the subpolar region, and one of its branches flows northeastward in direction of the Nordic Seas. This region is also characterized by the presence of the Rockall Trough (RT), in the north-east section of Figure 5.1a. The RT is a deep channel that allows the shallow poleward flow of saline water masses to penetrate into the Nordic seas. In this region these waters mix with the fresh waters coming from the west, forming waters of intermediate salinity. This region is important, because this poleward flow of water masses has an impact on deep convection, playing a key role in the thermohaline circulation.

Inside this region is also present an area in which two distinct water masses are formed: the Northeast Atlantic Deep Water (NEADW), and the Modified North Atlantic Water (MNAW). The former is a relatively high salinity and cold water mass that results from a mixture of local abyssal and intermediate water masses of high salinity coming from the Iceland-Scotland ridge and the Mediterranean water masses, at the south. The MNAW is a fresher water mass. The mixing occurs during winter-time when the mixed layer deepens. Both water masses are varieties of the Subpolar Mode Waters, that circulate cyclonically in the North Atlantic [Booth, 1988, Talley and McCartney, 1982, New and Smythe-Wright, 2001].

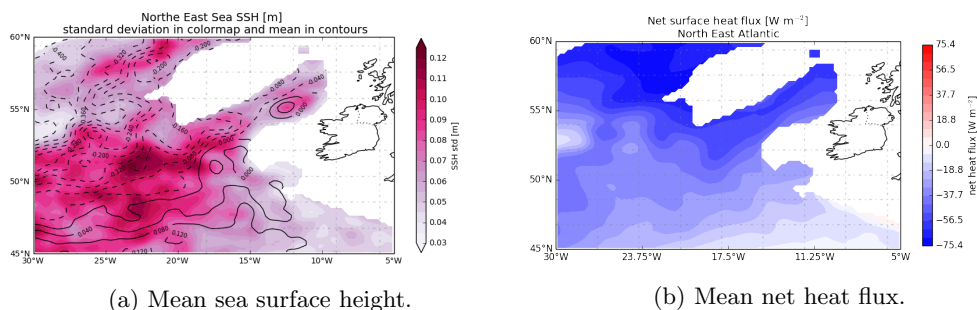


Figure 5.1: North East Atlantic: (a) Average and standard deviation of the sea surface height, SSH [m]. Contours represent the mean and color shading the standard deviation. (b) Net surface heat flux [ $\text{W m}^{-2}$ ]. Blue color shading represents flux out of the ocean and red flux into. Both fields computed over 2005-2018.

A general view of the surface circulation of the North East Atlantic region can be seen in the Figure 5.1a. This region is divided between a low and high SSH mean values, reflecting a

northeastward flow across the region. Also, the region presents areas of high SSH variability, reddish areas, related to eddy activity, as was pointed by [Booth, 1988]. In terms of net heat flux, Figure 5.1b, this region is characterized by a strong heat loss, mainly in the northern part, reaching  $-75.4 \text{ W m}^{-2}$ . At the south of this region the heat loss is small with magnitude close to  $-20 \text{ W m}^{-2}$ .

## 5.2 Mixed Layer characteristics and seasonal cycle

### 5.2.1 Mean and standard deviation

A time mean is computed over this area. The result is in Figure 5.2. The first thing that can be noticed is that the spatial distribution of the deep mixed layers values is shaped by the bathymetry (see Figure 7.2c). The deepest values are located in the northernmost areas. The high mixed layer depths values are all located where high standard deviation in MLD values are found. The MLD reaches a maximum of value  $(170 \pm 150) \text{ m}$  at  $(12^\circ\text{W}, 54^\circ\text{N})$ .

So far, it is difficult to distinguish a clear relationship between the mean SSH distribution and the mean MLD. This is also true for the SSH standard deviation and the MLD. Despite this, it is possible to notice that in the western area, at  $56^\circ\text{N}$ , there is a low SSH spot with relatively small standard deviation (Figure 5.1a). This coincides with the minimum MLD, also with very small variability (Figure 5.2).

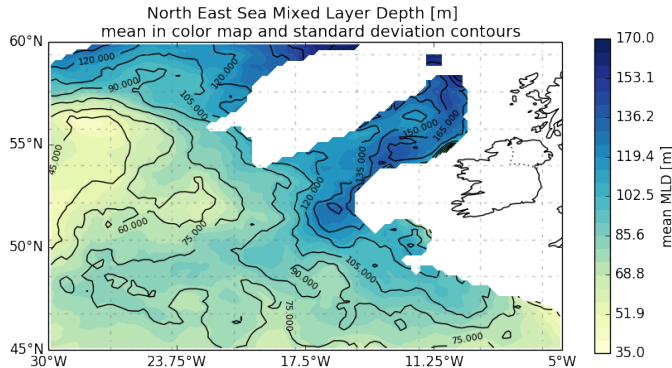


Figure 5.2: Time average and standard deviation of the Mixed Layer Depth, MLD [m]. The average is plotted in colormap and the standard deviation in contours, these quantities are computed in the 2005-2018 period.

### 5.2.2 Amplitude of the seasonal cycle

The mean amplitude of the seasonal cycle is plotted in Figure 5.3. The seasonal amplitude (Figure 4.3) and time mean of the mixed layer depth (Figure 5.2) share the same spatial distribution. Maximum values are found close to the continental slope, and especially high values north of the Rockall Trough. The maximum mean amplitudes reach 700 m, and the minimum are about 123 m. It can be inferred that the mixed layer depth in the entire region, has a strong seasonal variability.

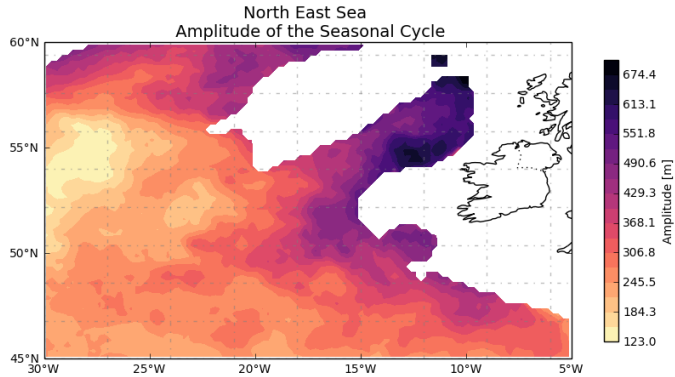


Figure 5.3: Mean amplitude of the seasonal cycle, in meters, computed for the years from 2005 to 2018.

## 5.3 Spatio-temporal statistics of the mixed layer depth

### 5.3.1 Dependence of seasonal cycle with latitude

To have an idea of how the mixed layer depth seasonal variability changes with latitude the Figure 5.4 was plotted. The first thing that can be said is that the seasonal cycle behaves the same across all the region. The main differences are due to the maximum values of MLD.

The maximum MLD values happen from December to March, having noticeable differences in the north-south direction. The maximum values increase poleward. This coincides with the characteristics previously described: deep mixed layer close to the continental slope generally located at northern positions.

In the northernmost section, between 56°N to 60°N, the region appears to have deeper mixed layers, having a maximum value extended in time, in the section north of 58.8°N. This maximum of 320 m starts at the beginning of February, when it also has its most southern extension and starts decaying in the first weeks of March. Going to the south, the maximum values start to decrease, reaching a maximum of 200 m.

The destratification process starts before in the north than in the south. It starts with almost one month of difference; September in the north, and October in the south. On the other hand, the stratification of the mixed layer starts in the last weeks of March reaching the minimum by late May. This is true for the complete region. The restratification is a faster process than the mixing. In this region, the former takes around three months, and the latter takes around six to seven months.

It is important to remember that this plot is related to space, therefore the plot can be a little misleading. For example, from Figure 5.2 it is evident that the maximum values are located around 55°N, in the Rockall Trough but in the zonal mean these deepest values seems to disappear due to the shallow MLD at the same latitude.

### 5.3.2 Mixed layer depth values distribution by seasons

The most abundant mixed layers are shallow, and they are in the range 12 m to 35 m. The main contributors are Summer and Spring. This range represents 50% of the MLD values of the region (Figure 5.5b). In the case of Autumn, it has its maximum at 55 m. Winter has its own clear peak near 200 m (Figure 3.6a).

Almost 90% of the grid points have MLD values inside the first 200 m, in Figure 5.5b). The seasons that contribute with more grid points are Spring, Winter and, in a smaller scale, Autumn.

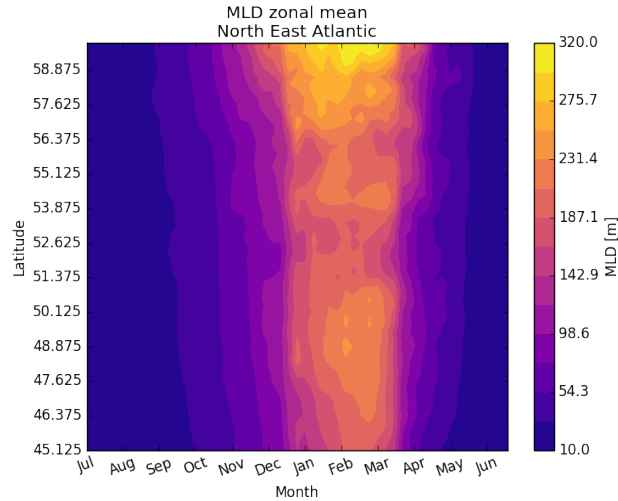


Figure 5.4: Zonal mean seasonal cycle of the MLD [m]. The mean is computed from weekly values for the years from 2005 to 2018.

The MLD values larger than 400 m are less of 3% of the total of grid points. The season that contributes the most in this range is Winter, see Figure 5.5a.

Looking for the differences between the histograms during the transition seasons (Figure 5.5a), Spring or Autumn, it is possible to know how the mixed layer varies from season to season. The maximum MLD increases from 150 m in Summer to 800 m in Autumn. The peak of the histograms also shifts to deeper values, from 20 m to 60 m. The number of grid points in the first bin also decreases in two orders of magnitude. Going from Autumn to Winter, the maximum MLD values are reached and the peak of the histograms shifts again. During Winter the peak of the histogram is at 160 m.

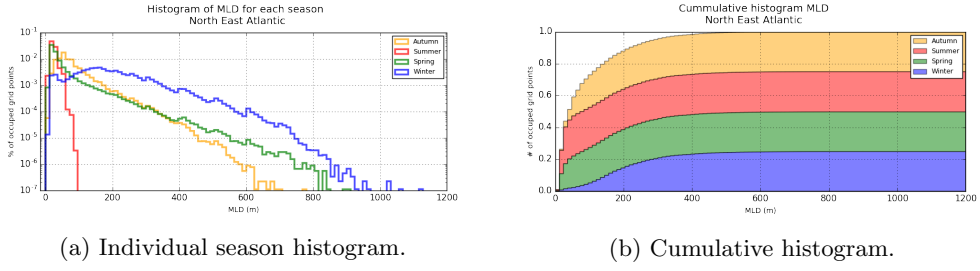
On the other hand, from Winter to Spring, the shape of the histogram is maintained. Especially beyond 200 m, the main difference is that the amount of grid points in this range is smaller in Spring than in Winter. This difference is compensated by the increase of the peak of the histogram for Spring, in the first 80 m. At this stage, the histogram starts to be more similar to the one for Summer. From Spring to Summer, the change in the histogram is sudden. All the grid points in the tail of the Spring histogram pass, mainly, to the peaks of Summer, located at 12 m and 35 m.

This difference in the transitions between Spring-Summer and Autumn-Winter can give an idea of the velocity of the mixing process of the surface layer of the ocean. The mixing takes a longer time to happen, as it was already pointed out, from Figure 5.4.

### 5.3.3 The seasonal cycle seen from the histograms

This region is characterized by a wide distribution, specially at the Autumn-Winter months. Other characteristic lies in the fact that the seasonal cycle has an impact in all the grid points' MLD. Said in other words: the regions' PDF maximum is always changing in depth and almost none grid point stays at shallow MLD values along the complete year. Another characteristic of this region is that during the January-April period the MLD concentration in deep values is more or less the same (figure 5.6).

In general terms, the seasonal cycle evolves as follows: the Winter time maximum around 160 m spotted in the previous section, is clear in January. In February this maximum spreads into deeper MLD values, as the tail of the histogram grows. During this time, the maximum depth is reached and maintained, until end of February when the MLD starts to shallow. Together with this shallowing, the histogram gets more compact too. This continues until the second part of



(a) Individual season histogram.

(b) Cumulative histogram.

Figure 5.5: (a) Normalized histogram of the MLD discriminated by seasons, in semi-log scale. (b) Normalized cumulative histogram for each one of the seasons. The seasons are identified by colors: Summer (red), Autumn (yellow), Winter (blue) and Spring (green). Both histograms consider each one of the 730 time steps in the 2005-2018 period, for the complete region. The total number of grid points is 3058152.

June and the beginning of July. In this period the distribution reaches the minimum MLD values and the peak is at its maximum. From the second part of July and the first middle of August, the MLD values start to get deeper, and therefore, more diverse. By Autumn, the histogram is already diversified.

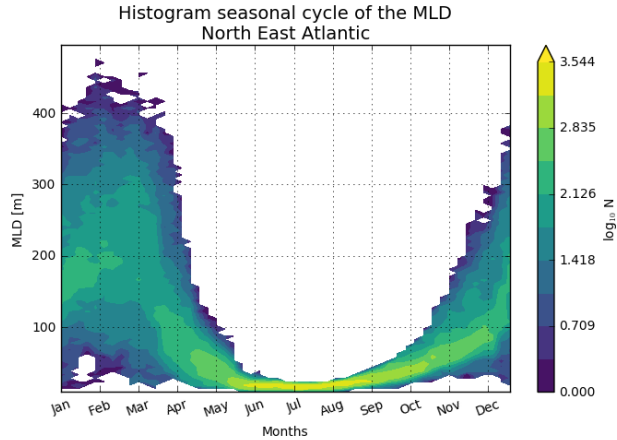


Figure 5.6: Seasonal cycle of the histograms over the North East Atlantic region, represented as weekly average over the period of 2005-2018. The x-axis is in months, y-axis is the Mixed Layer Depth. The colormap, in log scale, indicates the number of grid points  $N$  with a given MLD value.

## 5.4 Summary

The North East Atlantic region is characterized by a strong eddy activity, especially at its south-western area. The deep mixed layers are located along the continental slope, concentrated, principally, in the Rockall Trough. Is in this area where a maximum mean MLD is located, with magnitude of  $(170 \pm 165)$  m. The amplitude of the seasonal cycle has the same distribution as the time mean and standard deviation. The section in the Rockall Trough concentrates the larger amplitudes, in a range 430 m to 674 m. The smallest seasonal amplitude is reached in the western part of the region, with a value of 123 m. The differences of the seasonal cycle in latitudinal direction are mainly in the timing of the beginning and end of the mixing, and in the beginning and end of the restratification. In the section north of  $53^{\circ}\text{N}$  the mixing process starts in the first weeks

of September, and the maximum MLD is reached between February and March. The restratification in the northernmost position starts in March, finishing in mid-May. Therefore the mixing takes around 6 months and the restratification 3 months. In the south of 53°N the destratification starts in the first weeks of October, reaching the maximum MLD at the final of February, taking 5 months. The restratification starts in March and finishes in May, taking 3 months.

In this region, the most common mixed layer depths are in the range 15 m to 35 m. The changes Autumn-Winter and Winter-Spring seem to be gradual, meanwhile, the Spring-Summer transition is sudden. Up to the 90% of the grid points are MLD in the first 200 m. In this case, Summer and Spring are the seasons that contribute with most of these grid points. The maximum MLD reached in Summer is 95 m; in the other hand, the maximum value reached in Autumn is 800 m. Spring and Winter are more deep, with MLD larger than 1000 m.

# Chapter 6

## Nordic Sea

Please, note that here are considered the points whose bathymetry are deeper than 1000 m.

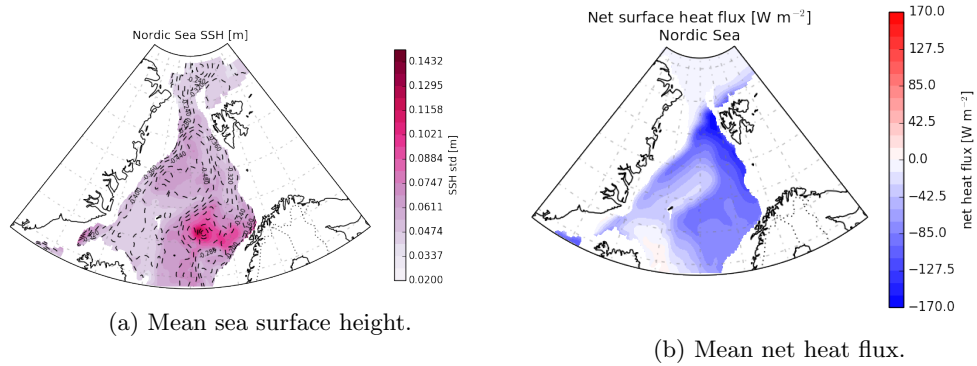


Figure 6.1: North East Atlantic: (a) Average and standard deviation of the sea surface height, SSH [m]. Contours represent the mean and color shading the standard deviation. (b) Net surface heat flux [ $\text{W m}^{-2}$ ]. Blue color shading represents flux out of the ocean and red flux into. Both fields computed over 2005-2018.

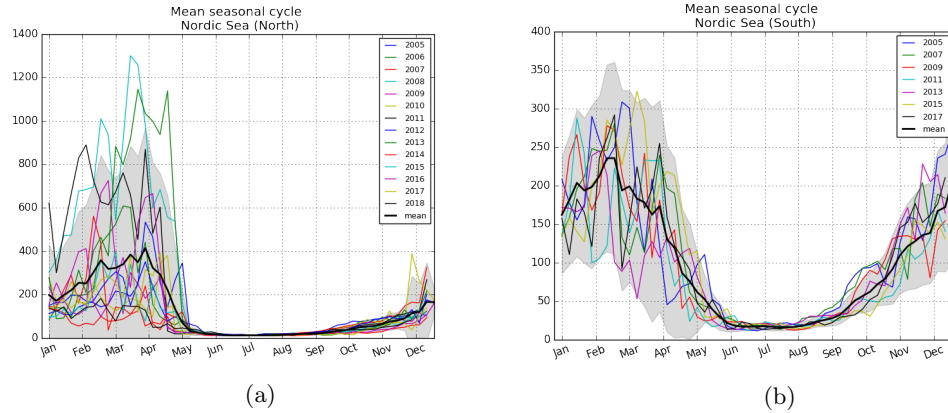


Figure 6.2: Mean seasonal cycle over the Nordic Sea sub-regions (in black) and standard deviation (gray shades). In colors the seasonal cycle for some years, inside each sub-region. (a) Sub-region centered at  $(0^{\circ}\text{E}, 75^{\circ}\text{N})$ . (b) Sub-region centered at  $(2^{\circ}\text{E}, 70^{\circ}\text{N})$ . The mean was computed over the 2005-2018 period.

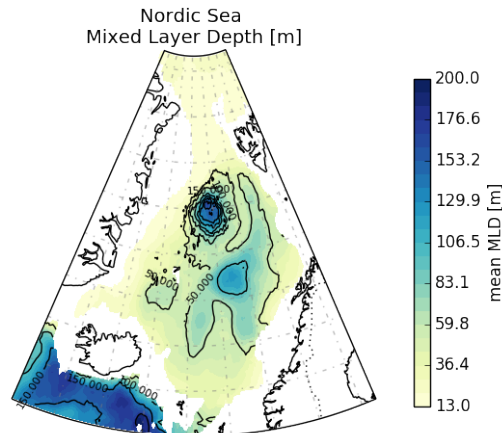


Figure 6.3: Time average and standard deviation of the Mixed Layer Depth, MLD [m]. The average is plotted in colormap and the standard deviation in contours, these quantities are computed in the 2005-2018 period.

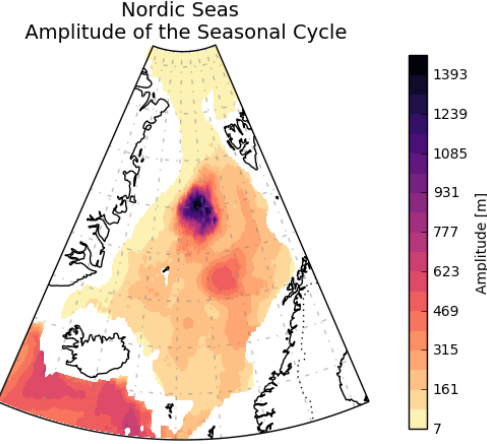


Figure 6.4: Mean amplitude of the seasonal cycle, in meters, computed for the years from 2005 to 2018.

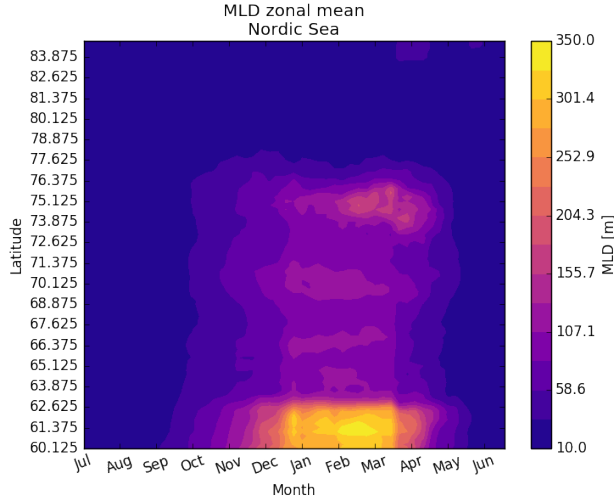


Figure 6.5: Zonal mean seasonal cycle of the MLD [m]. The mean is computed from weekly values for the years from 2005 to 2018.

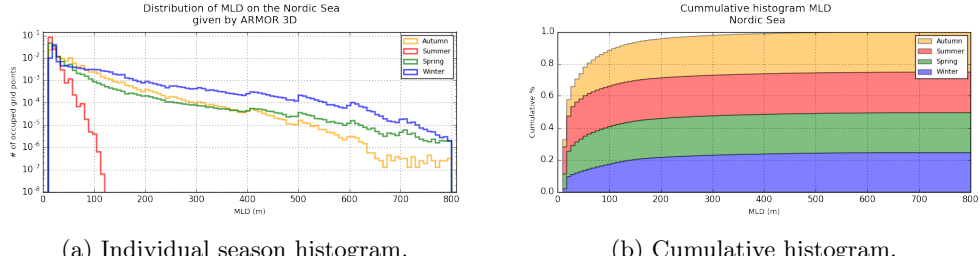


Figure 6.6: (a)Normalized histogram of the MLD discriminated by seasons, in semi-log scale. (b) Normalized cumulative histogram for each one of the seasons. The seasons are identified by colors: Summer (red), Autumn (yellow), Winter(blue) and Spring (green). Both histograms consider each one of the 730 time steps in the 2005-2018 period, for the complete region. The total number of grid points is 3058152.

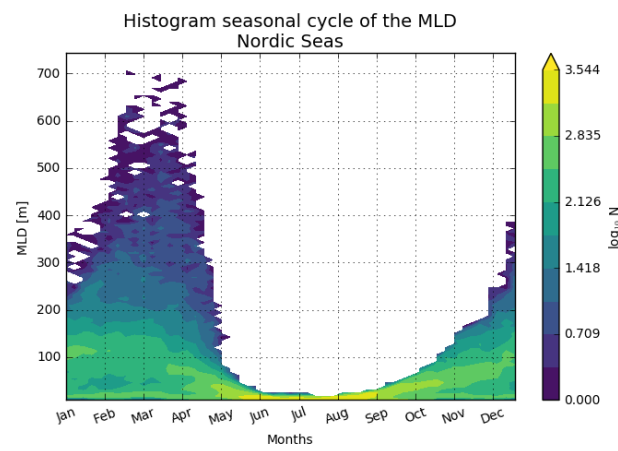


Figure 6.7: Seasonal cycle of the histograms over the Nordic Sea region, represented as weekly average over the period of 2005-2018. The x-axis is in months, y-axis is the Mixed Layer Depth. The colormap, in log scale, indicates the number of grid points  $N$  with a given MLD value.

# Chapter 7

## Discussion and Conclusions

We provided a description of the seasonal cycle of the mixed layer depth in three different regions of the North Atlantic Ocean: Gulf Stream, Labrador and Irminger Seas, and the North East Atlantic. Also, this project has allowed to take advantage of the high spatial and temporal resolution of the ARMOR 3D dataset.

Individually, each region has different circulation patterns, eddy activity and heat fluxes; imprinting distinctive characteristics and dynamics in the mixed layer depth seasonal cycle. This can be seen in Figures 7.1 and 7.2. The regions differ in the regional magnitude of MLD, including its interannual variability. Being the Gulf Stream the shallowest, with the smallest variability. In the case of the Labrador and Irminger Sea, although the regional mean is not the largest, the variability is. The North East presents the largest regional average MLD, but with a relative mild variability. This can be explained as a consequence of the spatial distribution of the MLD values, in Figure 7.2, where the maximum mixed layer depth is plotted. From this figure is clear that the three regions present a large spatial variability. Therefore, the resulting magnitude of the regional seasonal cycle; for example, the North East region, in Figure 7.2c, is dominated by relatively deep MLD values (around 300 m), with small clusters of shallower MLD. In contrast, the Labrador and Irminger Seas, Figure 7.2b, is dominated by shallow MLD values (around 20 m), yet in this region is reached the deepest MLD.

Furthermore, the regions with large eddy activity, Gulf Stream and North East Atlantic; tend to have a tighter spatial distribution of the MLD, Figures 3.7, 4.6, 5.6 and 7.2. All of the regions concentrate the deep mixed layer depth in hot spots, being in the Labrador sea clear that the location of this hot spot is related to the cyclonic circulation that is present in the region.

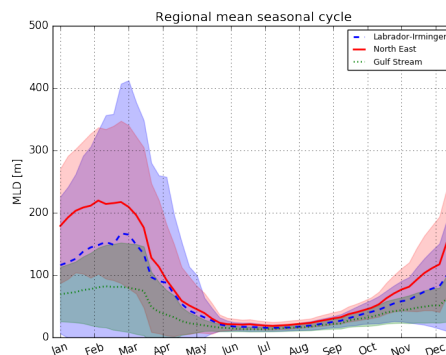


Figure 7.1: Regional mean seasonal cycle (line), and standard deviation (shades). Gulf Stream (green), Labrador and Irminger Seas (red), and North East Atlantic (blue). Mean and standard deviation are computed over 2005-2018 period.

Other common aspects of the seasonal cycle, shared by the regions, are: the coincidence of deep mixed layers in areas of relatively large heat loss, the time at which the maximum MLD happens, the constant presence of shallow MLD all along the year, and the duration of the destratification and restratification processes.

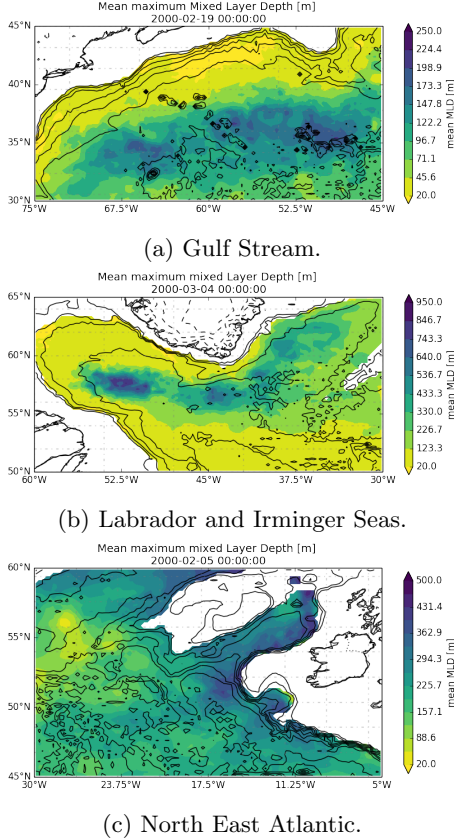


Figure 7.2: Maximum MLD, in the second week of February. Contours represent the bathymetry and color shading the mean MLD. (a) Gulf Stream, at Second week February; (b) Labrador and Irminger Seas, last week February; and (c) North East Atlantic, third week February.. Mean fields are computed over 2005-2018 period, the week for the maxima are taken from Figure 7.1

There is a difference in the speed at which the seasonal cycle of the mixed layer develops. For example, the deepening of the mixed layer takes between 8-6 months. It is longer in the Gulf Stream (8 months); for Labrador and Irminger Seas takes around 6 months and the North East takes between 6 to 7 months. The shoaling takes around 3 to 4 months, being longer in the North East region. Finally, the constant phase (and the minimum reacing) during Summer, takes from 1 to 3 months. The Labrador and Irminger region presents the longer of this phase, taking three months. This makes evident that solar isolation is one of the principal drivers of this variability, yet not the only one. This can be seen in Figures 3.5, 3.7; 4.4, 4.6; and 5.4, 5.6.

Despite the coincidence between the presence of deep mixed layers and the surface heat flux; the spatial distribution of maximum MLD values is not shared with the surface heat flux distribution. This is evident comparing Figures 3.1b, 4.1b and 5.1b with the correspondent mean mixed layer depth, in Figures 3.3, 4.2 and 5.2.

The timing in which the maximum MLD is reached in each area is also a common feature. All of them are reached in the final of February and first weeks of March, see Figures 3.5, 4.4 and 5.4 and 7.1. Slight differences in this timing are noticed going northward. The maximum is reached some weeks before in the regions that are located more to the north.

All of the regions presented shallow mixed layers along all the year, however, some differences between regions are noticeable. In the Labrador and Irminger Seas region, this minimum MLD values (first 35 m) are kept along all the year as the peak of the distribution 4.6. In the Gulf Stream the peak MLD peak of the distribution tends to change following the seasonal cycle 3.7. In this region the shallow MLD values are shifted, going from 10 m to 20 m during Autumn-Winter times. In the other hand, the North East the region presents a different behavior, in the sense that the distribution is more compact than in the other regions. This is: all the grid points experiment a change during the seasonal cycle. It can be seen in Figure 5.6, as the total absence of shallow MLD in the Autumn-Winter-Spring time, reaching the minimum MLD values only on Summer. This differences may be related to the eddy activity of the regions.

The shared characteristic of the seasonal cycle is the fast restratification, the slow destratification and the presence of a relatively constant phase of shallow mixed layers during Summer. Despite this similarities, the regions have their own singularities.

So far, this report has covered only the qualitative description of the seasonal cycle of the mixed layer depth over the selected regions. Hence, it is necessary to perform more quantitative studies. These further studies will be, then, oriented to complement the information here provided. Because of this, it will be desired to know how much of the temporal variability can be explained by the seasonal cycle. This can be achieved by the filtering of the signal of the seasonal cycle from the dataset time series. Once this relationship is found, it is necessary to know how much of the remaining temporal variability is introduced by the eddy activity, wind stress, and other variables. One approach for this is the computation of the temporal correlation of the variability of the MLD and the SSH. Additionally, the comparison of the average wind speed at the surface of the ocean with the MLD. Another parameter to explore is the relationship between surface sea temperature with the MLD. Furthermore, the rate of destratification and restratification should be measured; being one option to calculate the rate of change of the MLD, and look for the spatial distribution of this quantity.

One next step could be the simulation of the effects of any of these variables, e.g., the wind stress, on the MLD development under controlled boundary and initial conditions, without the forcing of other external factors. The development of probabilistic models that integrate the spatio-temporal variability of the MLD could be another approach too.



# Appendix A

## Description of ISAS dataset

ISAS stands for In Situ Analysis System, and it contains monthly grided fields of temperature and salinity syntetized from the ARGO datasets profiles of the same variables. This fields are projected on a horizontal grid of  $0.5^\circ$ . The version used in this work is the ISAS15, from the years 2006-2015 [Kolodziejczyk Nicolas, 2017].

In the case of the MLD, it is calculated using a fixed density criterion. In this work, we have available three different versions: ISAS-030, with  $0.030 \text{ kg m}^{-3}$ , ISAS-015 using with  $0.015 \text{ kg m}^{-3}$  and ISAS-046 with  $0.046 \text{ kg m}^{-3}$ . The nomenclature previously used for each ISAS version will be used in the following sections.

### A.1 Comparison of datasets

#### A.1.1 Mean Mixed Layer Depth

The first thing done was to compare the performance of the datasets by plotting the mean MLD over each one of the regions in the Atlantic Ocean (see Figure 1.2) using ARMOR 3D and ISAS (015, 030 and 046) datasets. The mean was computed in the 2006-2015 period for all datasets.

In general, it is easy to spot the effect that the density criteria has in the MLD: the larger is the threshold used, the larger the ML value.

In the Gulf Stream Extension region (Figure A.1) the position of the two MLD hot spots is slightly shifted. Using ARMOR 3D (Figure A.1a) as a reference, the hot spot at  $(63^\circ\text{W}, 35^\circ\text{N})$  is shifted to the west, close to  $69^\circ\text{W}$ . In the case of the maxima at  $(55^\circ\text{W}, 37^\circ\text{N})$ , it is shifted to the east, closer to  $52^\circ\text{W}$ . ISAS-015 is the version that has a mean MLD estimate closer to ARMOR 3D. Despite to keep some similarity in the distribution of the ML, ISAS fails<sup>1</sup> in the recreate the division between the north/south Gulf Stream MLD values. This is more evident with the two smaller criteria:  $0.015 \text{ kg m}^{-3}$  (Figure A.1c) and  $0.030 \text{ kg m}^{-3}$  (Figure A.1b). The largest threshold (Figure A.1d)reproduces in a better way the north/south distribution of MLD.

For the Labrador and Irminger seas (Figure A.2) the positions of the MLD maxima, at the Labrador and Irminger Seas respectively, are shifted northern-western than in ARMOR 3D version. In the three ISAS versions the Labrador's Sea maximum is overestimated. And is the same with the standard deviation values<sup>2</sup>.

In the case of the North East Atlantic (Figure A.3), the ISAS-015 dataset is the closest to ARMOR 3D. Nevertheless, this dataset fails to reproduce the magnitude of the MLD maximum located at, approximately,  $(15^\circ\text{W}, 68^\circ\text{N})$ . The division between shallow/deep ML from west to eats is well represented in 015 dataset, meanwhile in the remaining versions, this characteristic fades, having less shallow ML at the east.

<sup>1</sup>I do not know if is somehow fair to say it like this

<sup>2</sup>Does it have something to do with the temporal sampling?

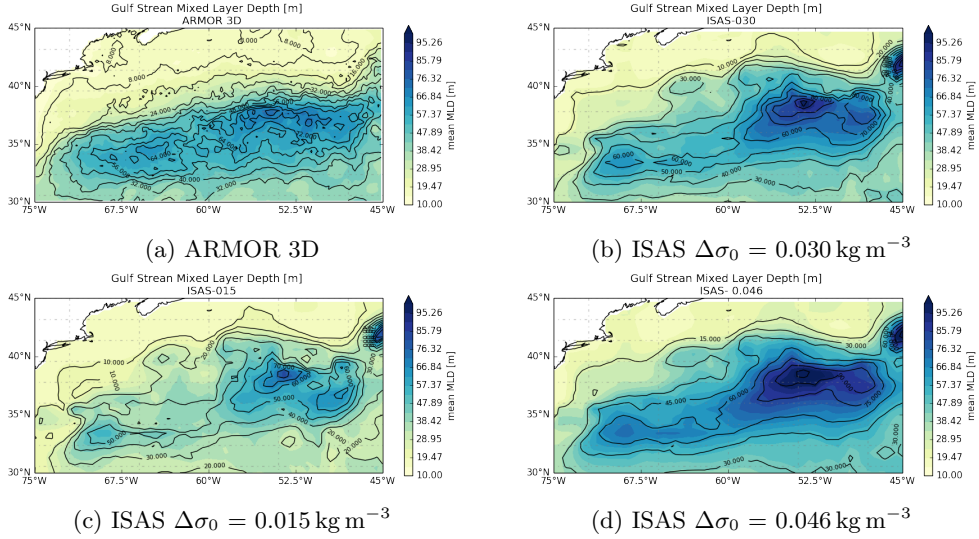


Figure A.1: Time average and standard deviation of the Mixed Layer Depth MLD [m] in the Gulf Stream Extension region. The average is plotted in colormap and the standard deviation in contours. The color bar covers the same range for all the plots. These quantities are computed in the period 2005-2018 for ARMOR, and 2002-2016 for ISAS. The three different plots for ISAS consider different criteria for the estimation of the MLD.

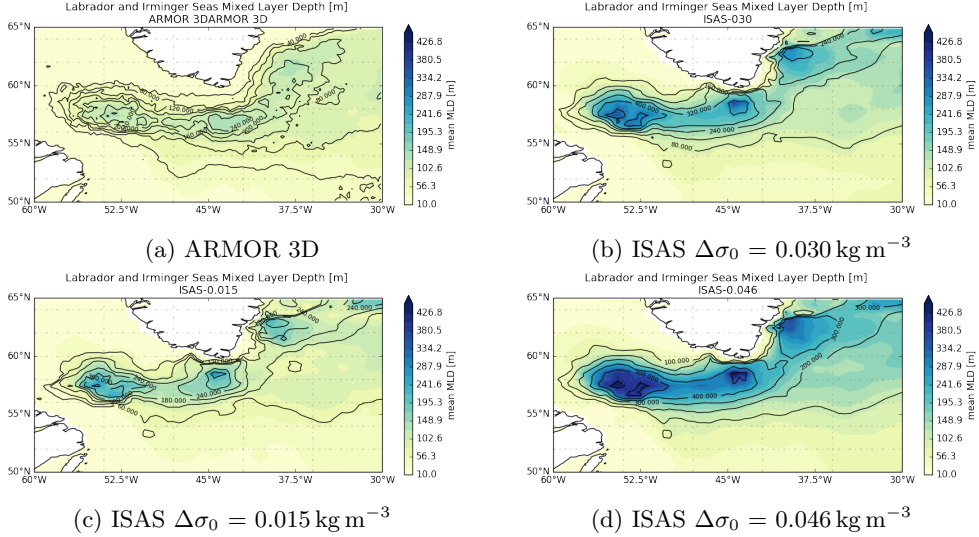


Figure A.2: Time average and standard deviation of the Mixed Layer Depth, MLD [m] in the Labrador and Irminger Seas region. The average is plotted in colormap and the standard deviation in contours. The color bar covers the same range in all the plots. These quantities are computed in the 2005-2018 (for ARMOR) and 2002-2016 (ISAS) period. Comparison of the estimation of MLD from ARMOR 3D and ISAS in the Nordic Seas. The three different plots for ISAS consider different criteria for the estimation of the MLD.

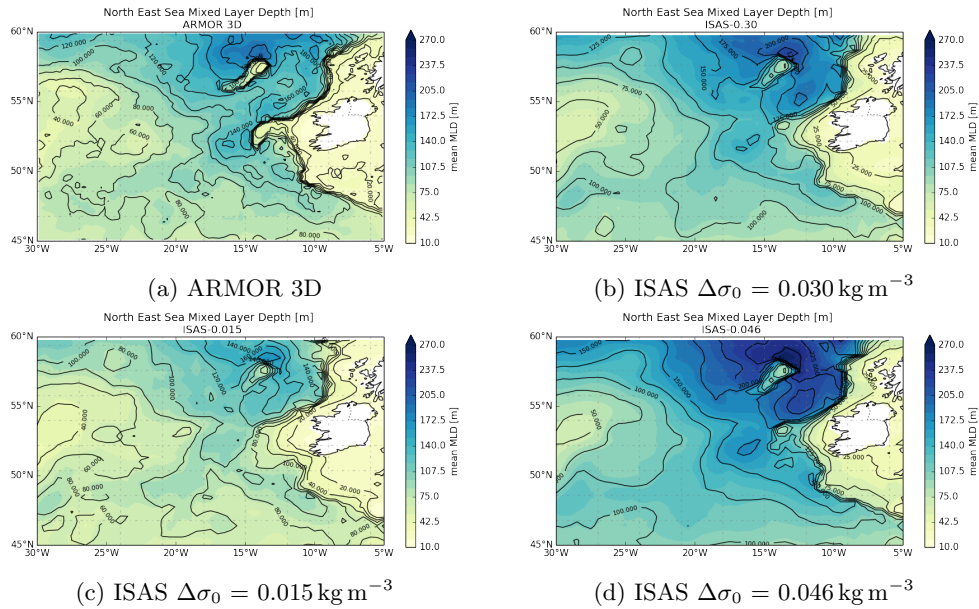


Figure A.3: Time average and standard deviation of the Mixed Layer Depth, MLD [m] in the North East Atlantic. The average is plotted in colormap and the standard deviation in contours. The color bar covers the same range in all the plots. These quantities are computed in the 2005-2018 (for ARMOR) and 2002-2016 (ISAS) period. Comparison of the estimation of MLD from ARMOR 3D and ISAS in the Nordic Seas. The three different plots for ISAS consider different criteria for the estimation of the MLD.

The Nordic Sea, in the other hand, the position of the MLD maximum at (5°W, 74°N) is well represented all ISAS versions. The magnitude and variability of this maximum is also changing from version to version. In the other hand, in the maximum located at (5°E, 70°N), in ARMOR 3D, is only defined in the ISAS-030 and ISAS-046. One important difference between ARMOR 3D and ISAS in this region is that in all ISAS versions a mean deep mixed layer spotted close to (10°W, 70°N). This maximum is accompanied by large variability, more noticeable in ISAS-030.

### A.1.2 Histograms, seasonal cycle

In this section the distribution of the mixed layer values in each season is evaluated. This is in Figures A.5, A.6, A.7 and A.8. The histograms are constructed on the 2006-2015 period for all datasets, and the histograms of each region are computed using different bin number.

In the Gulf Stream (Figure A.5), all the ISAS versions keep, in general, the same shape of the distribution for the four seasons. All ISAS versions are shallower than ARMOR 3D during Summer, and the same for Autumn. In the case of Spring, ISAS show a small amount of grid points with the largest values (larger than Winter). In the case of Winter, the maxima is displaced in one bin (with respect to ARMOR 3D), ISAS also present a slightly larger amount of grid points in the tail of the histograms.

Labrador and Irminger Seas (Figure A.6), all the ISAS datasets have a larger concentration of grid points in the deepest ML, for all the seasons. This concentration can reach one order of magnitude during Winter. It is also visible that ISAS reproduces a slightly more uniform distribution, specially in ISAS-030 and 046 (Winter and Spring). All ISAS dataset have the same MLD intervals along the region.

In contrast, the North East Atlantic region (Figure A.7) presents small differences in the range in which the MLD is represented in all the ISAS versions. This differences affect also to the deepest

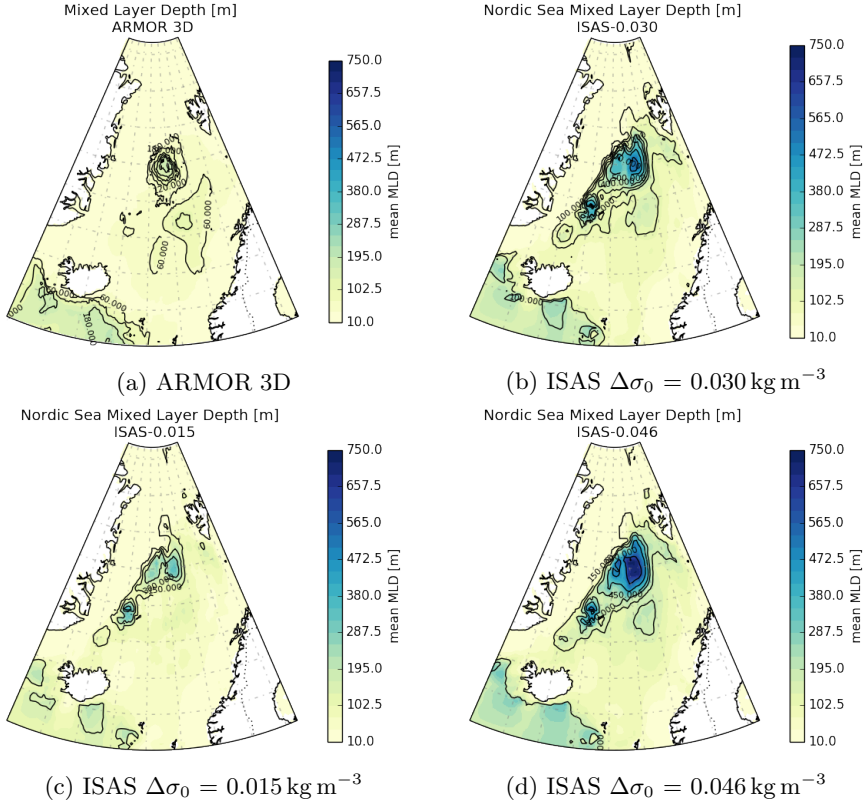


Figure A.4: Time average and standard deviation of the Mixed Layer Depth, MLD [m] in the Nordic Sea. The average is plotted in colormap and the standard deviation in contours. The color bar covers the same range in all the plots. These quantities are computed in the 2005-2018 (for ARMOR) and 2002-2016 (ISAS) period. Comparison of the estimation of MLD from ARMOR 3D and ISAS in the Nordic Seas. The three different plots for ISAS consider different criteria for the estimation of the MLD.

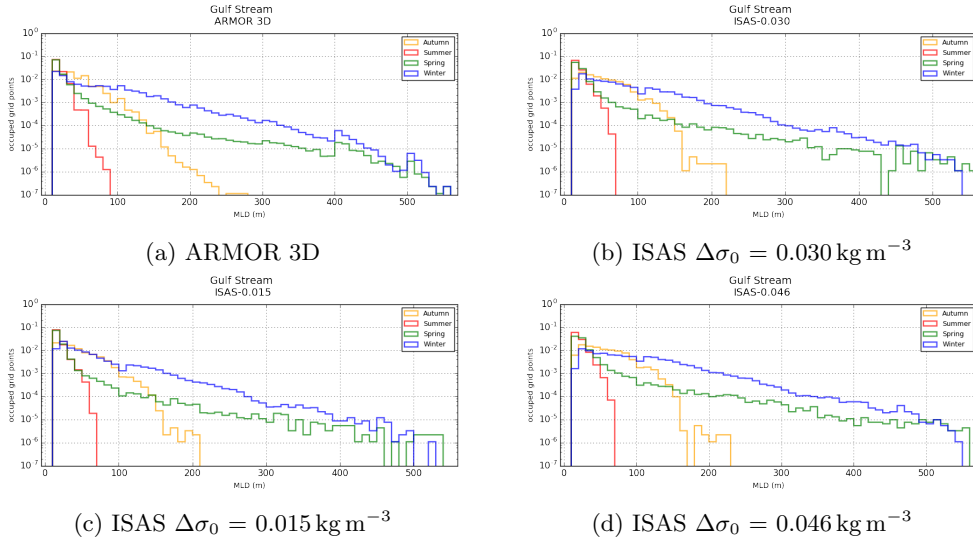


Figure A.5: Normalized histogram of the MLD discriminated by seasons, in semi-log scale for the Gulf Stream extension region. The seasons are identified by colors: Summer (red), Autumn (yellow), Winter(blue) and Spring (green). Both histograms consider each one of the time steps in the 2006-2015 period, for the complete region. The number of bins is 55.

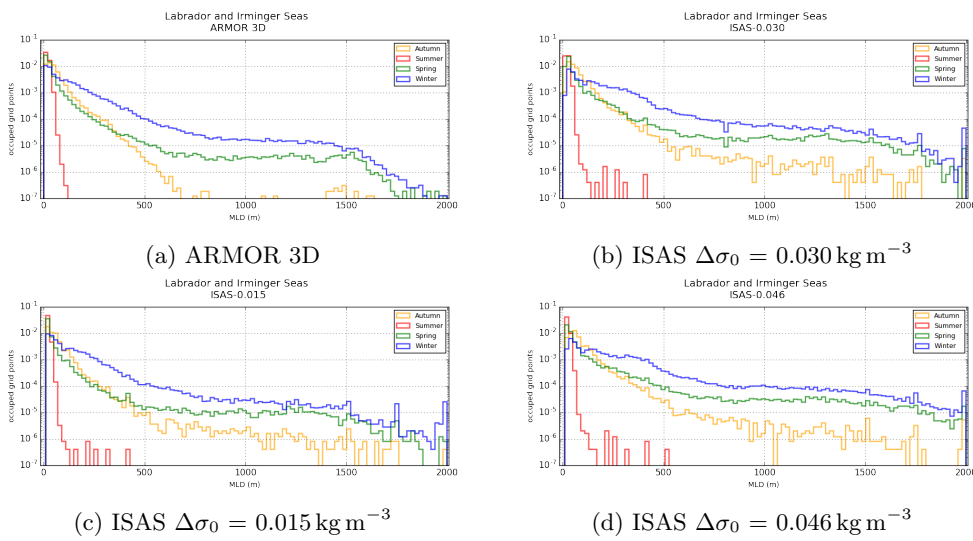


Figure A.6: Normalized histogram of the MLD discriminated by seasons, in semi-log scale for the Labrador and Irminger region. The seasons are identified by colors: Summer (red), Autumn (yellow), Winter(blue) and Spring (green). Both histograms consider each one of the time steps in the 2006-2015 period, for the complete region. The number of bins is 100.

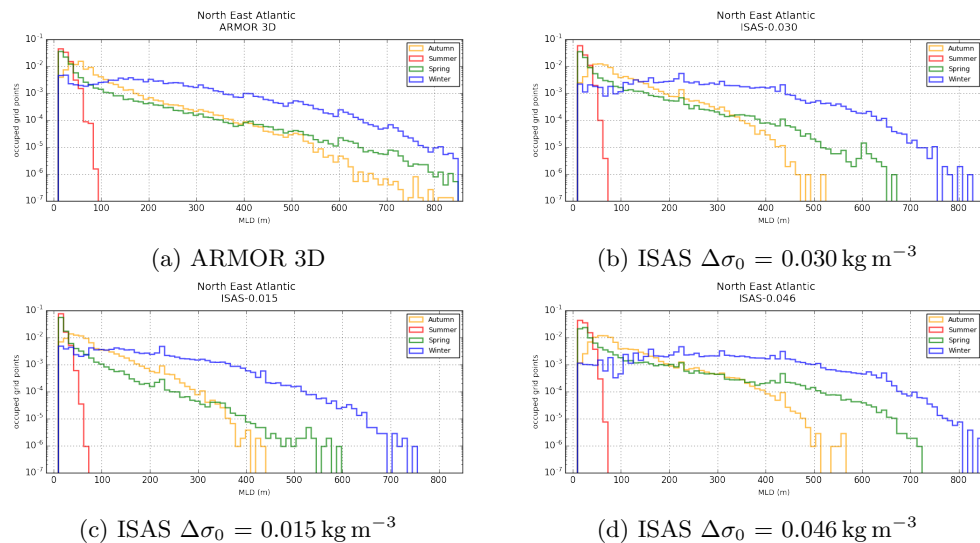


Figure A.7: Normalized histogram of the MLD discriminated by seasons, in semi-log scale for the North East Atlantic region. The seasons are identified by colors: Summer (red), Autumn (yellow), Winter(blue) and Spring (green). Both histograms consider each one of the time steps in the 2006-2015 period, for the complete region. Number of bins: 80.

values reached during Autumn, Winter and Spring; see Figures A.7a and A.7c in which, despite being the most similar representations, the small threshold in ISAS-015 affects the deepest value that is possible to find in the region. In the other hand, in ISAS-046 (even ISAS-030) the large threshold value are the reason of the larger population of ML in deep values, while it is also the cause of the loss of grid points in the shallow MLD (Figures A.7b and A.7d). This loose and gain of grid points between shallow and deep ML is more evident in the Winter histograms for both datasets.

For the Nordic Seas, in Figure A.8, the MLD distributions given by all the ISAS versions are very similar. All the datasets give the same MLD upper limit. The main differences between the distribution given by ARMOR 3D and all ISAS happen in the Winter and Autumn histograms. In all the ISAS versions there is present a small overestimation of deep mixed layers which causes a larger amount of grid points in the deep ML values. This is more evident in the ISAS-046, Figure A.8d, where the amount of deep Winter values is so high that the first bin of this histogram is smaller than in the ISAS-015 and ISAS-030 versions (Figures A.8c and Figure A.8b).

### A.1.3 Seasonal cycles

The monthly seasonal cycles inside each of the sub-regions, illustrated in Figure 1.3, they were calculated over the 2006-2015 period.

ISAS datasets have smaller variability in the Gulf Stream, Figure A.9, specially in the summer period. In the winter months the variability is larger. Other characteristic of the ISAS datasets is that the shoaling of the ML has a steeper slope. Also, during the summer, the MLD is almost set at the same value being totally constant from May to July. This characteristic is more evident in ISAS-015 (Figure A.9c). In the other hand, the ISAS-030 version is the one whose seasonal cycle is more similar to the ARMOR 3D. This similarity is mainly in the magnitude.

In the case of the Labrador Sea (Figure A.10) it is noticeable that the MLD is overestimated in all ISAS versions. This happens mostly in the winter months, where also the variability is large. In the case of the Summer-Autumn months, all datasets reproduce approximately the same magnitude and variability of MLD. It is also evident that the datasets overestimate the ML cycle

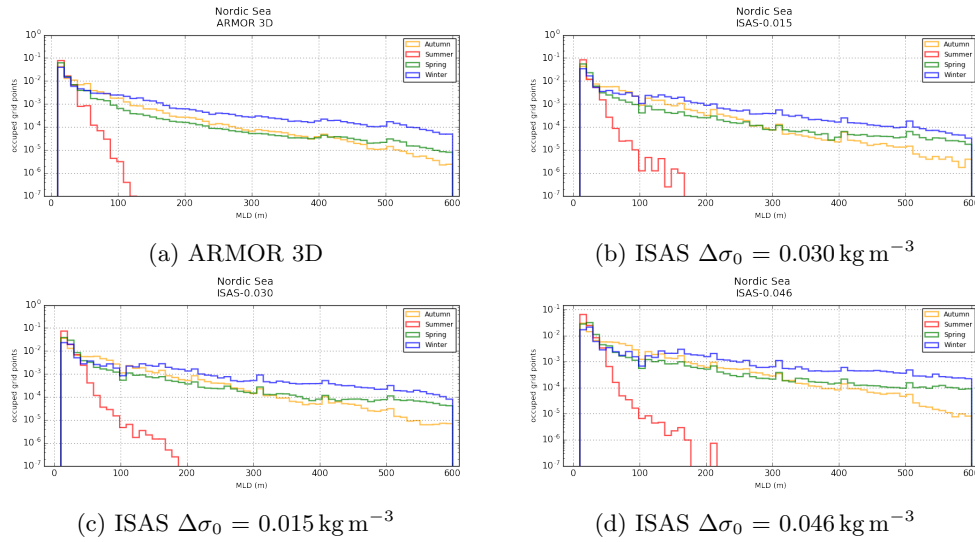


Figure A.8: Normalized histogram of the MLD discriminated by seasons, in semi-log scale for the Nordic Sea region. The seasons are identified by colors: Summer (red), Autumn (yellow), Winter(blue) and Spring (green). Both histograms consider each one of the time steps in the 2006-2015 period, for the complete region.

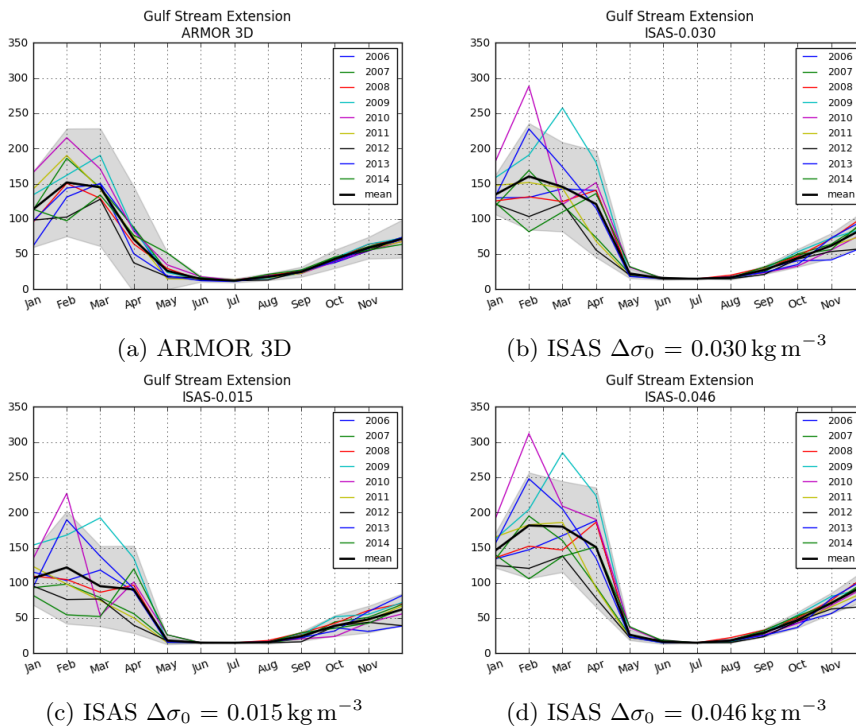


Figure A.9: Mean seasonal cycle over the Gulf Stream Extension sub-regions (in black) and standard deviation (gray shades). In color seasonal cycle for some years. The mean was computed over the 2006-2015 period. (a) Monthly ARMOR 3D, (b) ISAS-030, (c) ISAS-015 and (d) ISAS-046. Number of bins: 60.

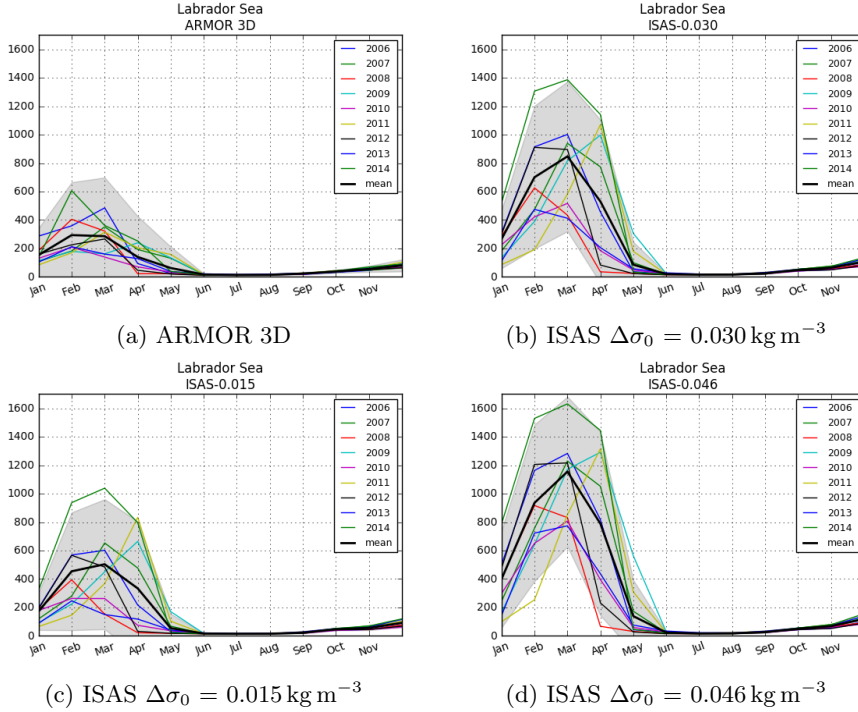


Figure A.10: Mean seasonal cycle over the Labrador Sea sub-regions (in black) and standard deviation (gray shades). In color seasonal cycle for some years. The mean was computed over the 2006-2015 period. (a) Monthly ARMOR 3D, (b) ISAS-030, (c) ISAS-015 and (d) ISAS-046.

in the year 2014. Although it is not the same magnitude it has the same shape in all versions of ISAS; in ARMOR this same year is the one that reaches the maximum MLD of all years, but it is only present in February, being the rest of the winter values considered as 'normal'.

In the other hand, the ISAS datasets (Figure A.11) have a different behaviour in the Irminger Sea. This is in the sense that the density criteria has strong influence in the shape and magnitude of the seasonal cycle. This effect is diverse, but it can be seen that the increase of the criteria increases also the variability, specially in the Winter-Spring months. In this sub-region ISAS-030 (Figure A.11b) replicates the shape of the seasonal cycle but it overestimates the magnitude of the MLD. Nevertheless, this is the version that better matches to the ARMOR 3D monthly estimation.

ISAS datasets also reproduce a less variable ML in the North East Atlantic sub-region (Figure A.12). This small variability can be noticed along all the year in the three versions of ISAS. Also, ISAS-030 is the version that matches better the ARMOR 3D seasonal cycle.

In the case of the Nordic Seas North sub-region (Figure A.13) All ISAS datasets overestimate the magnitude of the seasonal cycle, specially in winter and spring months. The variability is also very large during Winter. In this case, ISAS-015 is the (Figure A.13c) that reproduces more accurately the seasonal cycle. For the sub-region Nordic Sea South (Figure A.14) the overestimation is also present, specially in the versions 030 and 046 (Figures A.14b and A.14d). Despite the overestimation, the variability of the all ISAS datasets is smaller than for ARMOR 3D, even during the Winter and Spring months. In all datasets the maximum is shifted one month, in comparison with ARMOR 3D; happening in March. Overall, in this sub-region ISAS-015 (Figure A.14c) reproduces a seasonal cycle more similar to ARMOR 3D.

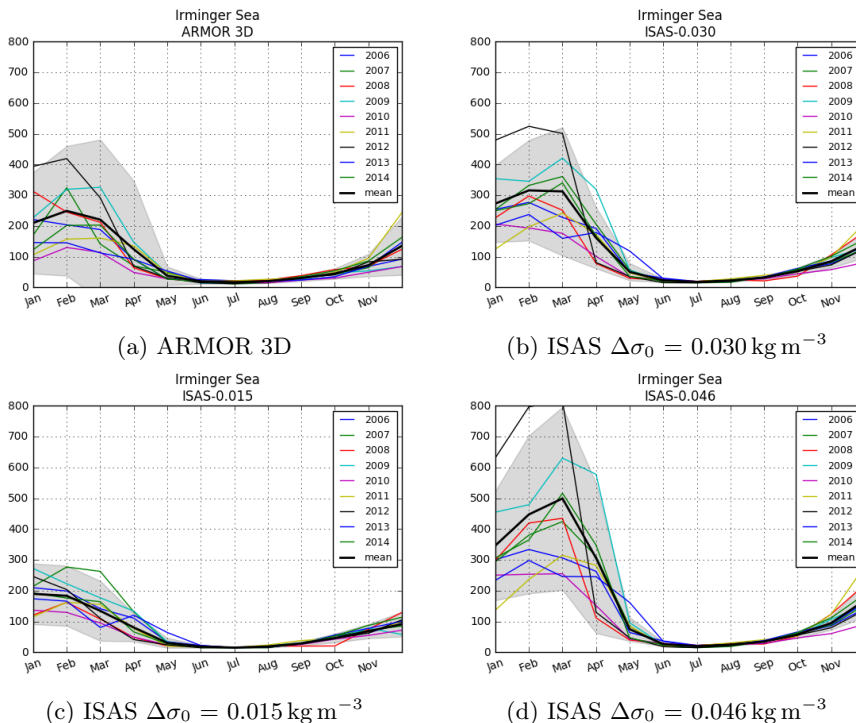


Figure A.11: Mean seasonal cycle over the Irminger Sea Extension sub-regions (in black) and standard deviation (gray shades). In color seasonal cycle for some years. The mean was computed over the 2006-2015 period. (a) Monthly ARMOR 3D, (b) ISAS-030, (c) ISAS-015 and (d) ISAS-046.

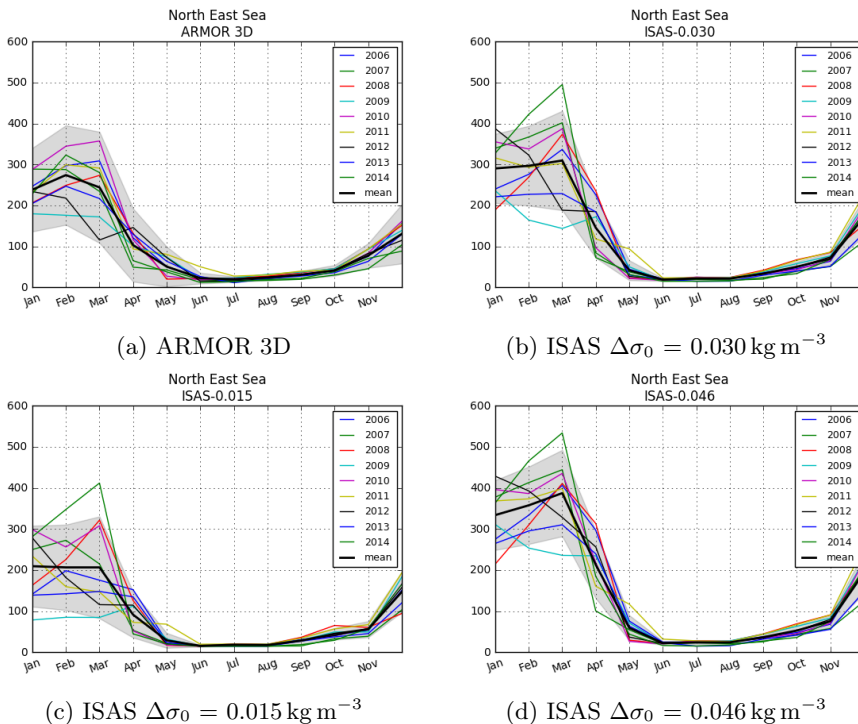


Figure A.12: Mean seasonal cycle over the South Rockall Trough Extension sub-regions (in black) and standard deviation (gray shades). In color seasonal cycle for some years. The mean was computed over the 2006-2015 period. (a) Monthly ARMOR 3D, (b) ISAS-030, (c) ISAS-015 and (d) ISAS-046.

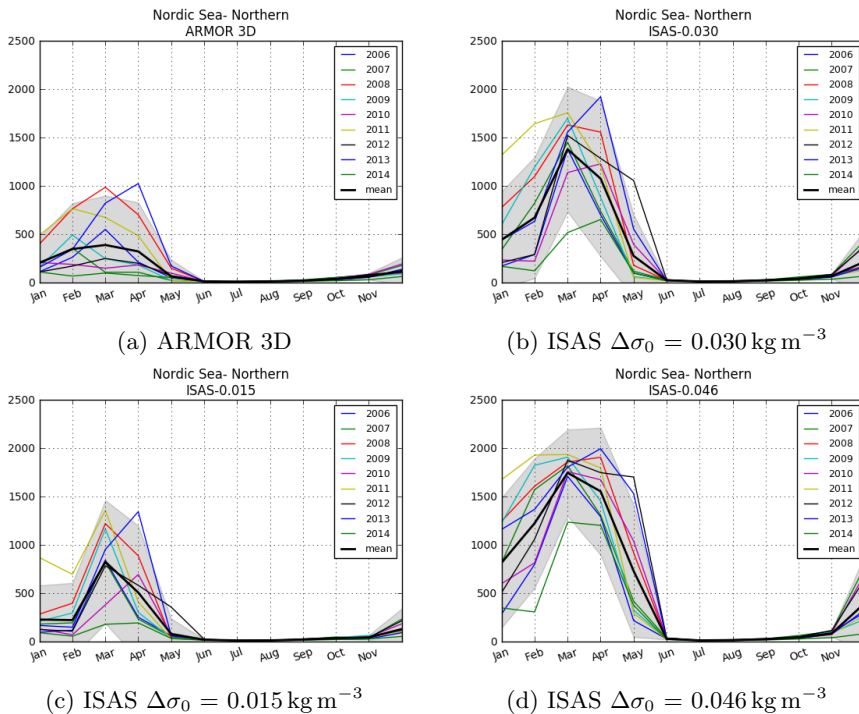


Figure A.13: Mean seasonal cycle over the Nordic Sea North Extension sub-regions (in black) and standard deviation (gray shades). In color seasonal cycle for some years. The mean was computed over the 2006-2015 period. (a) Monthly ARMOR 3D, (b) ISAS-030, (c) ISAS-015 and (d) ISAS-046.

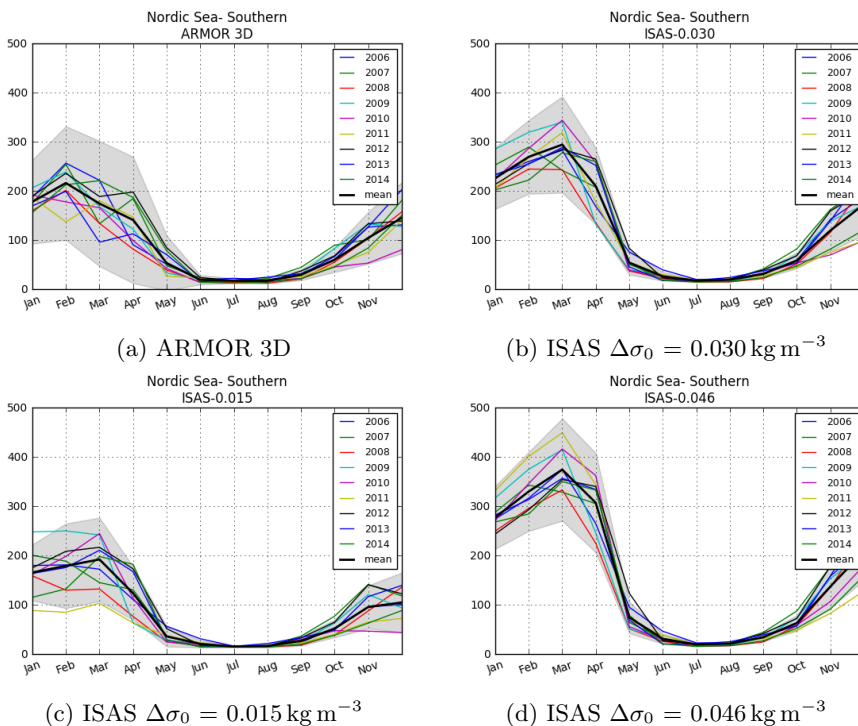


Figure A.14: Mean seasonal cycle over the Nordic Sea South Extension sub-regions (in black) and standard deviation (gray shades). In color seasonal cycle for some years. The mean was computed over the 2006-2015 period. (a) Monthly ARMOR 3D, (b) ISAS-030, (c) ISAS-015 and (d) ISAS-046.

# Bibliography

- [Bacon et al., 2003] Bacon, S., Gould, W. J., and Jia, Y. (2003). Open-ocean convection in theirminger sea. *Geophysical Research Letters*, 30(5).
- [Booth, 1988] Booth, D. A. (1988). Eddies in the rockall trough. *Oceanologica acta*, 11(3):213–219.
- [de Boyer Montégut et al., 2004] de Boyer Montégut, C., Madec, G., Fischer, A. S., Lazar, A., and Iudicone, D. (2004). Mixed layer depth over the global ocean: An examination of profile data and a profile-based climatology. *Journal of Geophysical Research: Oceans*, 109(C12).
- [Gaube et al., 2019] Gaube, P., J. McGillicuddy Jr, D., and Moulin, A. J. (2019). Mesoscale eddies modulate mixed layer depth globally. *Geophysical Research Letters*, 46(3):1505–1512.
- [Group, 2020] Group, G. C. (2020). Gebco 2020 grid.
- [Guinehut et al., 2012] Guinehut, S., Dhomps, A.-L., Larnicol, G., and Le Traon, P.-Y. (2012). High resolution 3-d temperature and salinity fields derived from in situ and satellite observations. *Ocean Science*, 8(5):845–857.
- [Holte et al., 2017] Holte, J., Talley, L. D., Gilson, J., and Roemmich, D. (2017). An argo mixed layer climatology and database. *Geophysical Research Letters*, 44(11):5618–5626.
- [Joyce, 2011] Joyce, T. M. (2011). New perspectives on eighteen-degree water formation in the north atlantic. In *New Developments in Mode-Water Research*, pages 41–48. Springer.
- [Kantha and Clayson, 2003] Kantha, L. and Clayson, C. (2003). Boundary layers — ocean mixed layer. In Holton, J. R., editor, *Encyclopedia of Atmospheric Sciences*, pages 291 – 298. Academic Press, Oxford.
- [Kolodziejczyk Nicolas, 2017] Kolodziejczyk Nicolas, Prigent-Mazella Annaig, G. F. (2017). Isas-15 temperature and salinity gridded fields.
- [Lazier et al., 2002] Lazier, J., Hendry, R., Clarke, A., Yashayaev, I., and Rhines, P. (2002). Convection and restratification in the labrador sea, 1990–2000. *Deep Sea Research Part I: Oceanographic Research Papers*, 49(10):1819 – 1835.
- [McCulloch et al., 2004] McCulloch, M., Alves, J., and Bell, M. (2004). Modelling shallow mixed layers in the northeast atlantic. *Journal of Marine Systems*, 52(1):107 – 119.
- [Monterey and Levitus, 1997] Monterey, G. I. and Levitus, S. (1997). *Seasonal variability of mixed layer depth for the world ocean*. US Department of Commerce, National Oceanic and Atmospheric Administration.
- [New and Smythe-Wright, 2001] New, A. and Smythe-Wright, D. (2001). Aspects of the circulation in the rockall trough. *Continental Shelf Research*, 21(8):777 – 810. The Marine Environment of the North East Atlantic Margin.

- [Pickart et al., 2003] Pickart, R. S., Straneo, F., and Moore, G. K. (2003). Is labrador sea water formed in the irminger basin? *Deep Sea Research Part I: Oceanographic Research Papers*, 50(1):23–52.
- [Piron et al., 2016] Piron, A., Thierry, V., Mercier, H., and Caniaux, G. (2016). Argo float observations of basin-scale deep convection in the irminger sea during winter 2011–2012. *Deep Sea Research Part I: Oceanographic Research Papers*, 109:76 – 90.
- [Schiller and Ridgway, 2013] Schiller, A. and Ridgway, K. R. (2013). Seasonal mixed-layer dynamics in an eddy-resolving ocean circulation model. *Journal of Geophysical Research: Oceans*, 118(7):3387–3405.
- [Siedler et al., 2013] Siedler, G., Griffies, S., Gould, J., and Church, J., editors (2013). *Ocean Circulation and Climate: a 21st Century perspective. 2nd Ed.* 103. Academic Press.
- [Talley, 2011] Talley, L. (2011). *Descriptive Physical Oceanography: An Introduction*. Elsevier Science.
- [Talley, 1996] Talley, L. D. (1996). North atlantic circulation and variability, reviewed for the cnls conference. *Physica D: Nonlinear Phenomena*, 98(2):625 – 646. Nonlinear Phenomena in Ocean Dynamics.
- [Talley and McCartney, 1982] Talley, L. D. and McCartney, M. S. (1982). Distribution and Circulation of Labrador Sea Water. *Journal of Physical Oceanography*, 12(11):1189–1205.
- [Toyoda et al., 2017] Toyoda, T., Fujii, Y., Kuragano, T., Kamachi, M., Ishikawa, Y., Masuda, S., Sato, K., Awaji, T., Hernandez, F., Ferry, N., et al. (2017). Intercomparison and validation of the mixed layer depth fields of global ocean syntheses. *Climate Dynamics*, 49(3):753–773.
- [Verbrugge et al., 2019] Verbrugge, N., Mulet, S., Guinehut, S., Buongiorno Nardelli, B., and Droghei, R. (2019). Quality information document, for global ocean multi observation products: Multiobs\_glo\_phy\_rep\_015\_002.